

**Mitochondrial respiratory states and rates:
Building blocks of mitochondrial physiology
Part 1.**

http://www.mitoeagle.org/index.php/MitoEAGLE_preprint_2018-02-08

Preprint version 25 (2018-02-16)

MitoEAGLE Network

Corresponding author: Gnaiger E

Contributing co-authors

Acuna-Castroviejo D, Ahn B, Alves MG, Amati F, Aral C, Arandarčikaitė O, Åsander Frostner E, Bailey DM, Bastos Sant'Anna Silva AC, Battino M, Beard DA, Ben-Shachar D, Bishop D, Borutaitė V, Breton S, Brown GC, Brown RA, Buettner GR, Calabria E, Cardoso LHD, Carvalho E, Casado Pinna M, Cervinkova Z, Chang SC, Chen Q, Chicco AJ, Chinopoulos C, Coen PM, Collins JL, Crisóstomo L, Davis MS, Dias T, Distefano G, Doerrier C, Drahota Z, Duchen MR, Ehinger J, Elmer E, Endlicher R, Fell DA, Ferko M, Ferreira JCB, Filipovska A, Fisar Z, Fisher J, Garcia-Roves PM, Garcia-Souza LF, Genova ML, Gonzalo H, Goodpaster BH, Gorr TA, Grefte S, Han J, Harrison DK, Hellgren KT, Hernansanz P, Holland O, Hoppel CL, Houstek J, Hunger M, Iglesias-Gonzalez J, Irving BA, Iyer S, Jackson CB, Jadiya P, Jansen-Dürr P, Jespersen NR, Jha RK, Kaambre T, Kane DA, Kappler L, Karabatsiakakis A, Keijer J, Keppner G, Komlodi T, Kopitar-Jerala N, Krako Jakovljevic N, Kuang J, Kucera O, Labieniec-Watala M, Lai N, Laner V, Larsen TS, Lee HK, Lemieux H, Lerfall J, Lucchinetti E, MacMillan-Crow LA, Makrecka-Kuka M, Meszaros AT, Michalak S, Moiso N, Molina AJA, Montaigne D, Moore AL, Moreira BP, Mracek T, Muntane J, Muntean DM, Murray AJ, Nedergaard J, Nemec M, Newsom S, Nozickova K, O'Gorman D, Oliveira PF, Oliveira PJ, Orynbayeva Z, Pak YK, Palmeira CM, Patel HH, Pecina P, Pereira da Silva Grilo da Silva F, Pesta D, Petit PX, Pichaud N, Pirkmajer S, Porter RK, Pranger F, Prochownik EV, Puurand M, Radenkovic F, Reboredo P, Renner-Sattler K, Robinson MM, Rohlena J, Røslund GV, Rossiter HB, Rybacka-Mossakowska J, Saada A, Salvadego D, Scatena R, Schartner M, Scheibye-Knudsen M, Schilling JM, Schlattner U, Schoenfeld P, Scott GR, Shabalina IG, Sharma P, Shevchuk I, Siewiera K, Singer D, Sobotka O, Sokolova I, Spinazzi M, Stankova P, Stier A, Stocker R, Sumbalova Z, Suravajhala P, Tanaka M, Tandler B, Tepp K, Tomar D, Towheed A, Tretter L, Trivigno C, Tronstad KJ, Trougakos IP, Tyrrell DJ, Urban T, Valentine JM, Velika B, Vendelin M, Vercesi AE, Victor VM, Villena JA, Wagner BA, Ward ML, Watala C, Wei YH, Wieckowski MR, Wohlwend M, Wolff J, Wuest RCI, Zaugg K, Zaugg M, Zorzano A

Supporting co-authors:

Bakker BM, Bernardi P, Boetker HE, Borsheim E, Bouitbir J, Calbet JA, Calzia E, Chaurasia B, Clementi E, Coker RH, Collin A, Das AM, De Palma C, Dubouchaud H, Durham WJ, Dyrstad SE, Engin AB, Fischer M, Fornaro M, Gan Z, Garlid KD, Garten A, Gourlay CW, Granata C, Haas CB, Haavik J, Haendeler J, Hand SC, Hepple RT, Hickey AJ, Hoel F, Jang DH, Kainulainen H, Khamoui AV, Klingenspor M, Koopman WJH, Kowaltowski AJ, Krajcova A, Lane N, Lenaz G, Malik A, Markova M, Mazat JP, Menze MA, Methner A, Neuzil J, Oliveira MT, Pallotta ML, Parajuli N, Pettersen IKN, Porter C, Pulinilkunnil T, Ropelle ER, Salin K, Sandi C, Sazanov LA, Schwarzer C, Silber AM, Skolik R, Smenes BT, Soares FAA, Sonkar VK, Swerdlow RH, Szabo I, Trifunovic A, Thyfault JP, Vieyra A, Votion DM, Williams C, Zischka H

Updates and discussion:

http://www.mitoeagle.org/index.php/MitoEAGLE_preprint_2018-02-08

Correspondence: Gnaiger E

Chair COST Action CA15203 MitoEAGLE – <http://www.mitoeagle.org>

Department of Visceral, Transplant and Thoracic Surgery, D. Swarovski Research
Laboratory, Medical University of Innsbruck, Innrain 66/4, A-6020 Innsbruck, Austria

Email: erich.gnaiger@i-med.ac.at

Tel: +43 512 566796, Fax: +43 512 566796 20

Contents**Abstract****Executive summary****1. Introduction** – Box 1: In brief: Mitochondria and Bioblasts**2. Oxidative phosphorylation and coupling states in mitochondrial preparations**

Mitochondrial preparations

2.1. Respiratory control and coupling

The steady-state

Specification of biochemical dose

Phosphorylation, P_{\gg} , and P_{\gg}/O_2 ratio

Control and regulation

Respiratory control and response

Respiratory coupling control and ET-pathway control

Coupling

Uncoupling

2.2. Coupling states and respiratory rates

Respiratory capacities in coupling control states

LEAK, OXPHOS, ET, ROX

2.3. Classical terminology for isolated mitochondria

States 1–5

3. Normalization: fluxes and flows*3.1. Normalization: system or sample*

Flow per system, I

Extensive quantities

Size-specific quantities – Box 2: Metabolic fluxes and flows: vectorial and scalar

3.2. Normalization for system-size: flux per chamber volume

System-specific flux, J

3.3. Normalization: per sample

Sample concentration, C_{mX}

Mass-specific flux, J_{mX,O_2}

Number concentration, C_{NX}

Flow per object, I_{X,O_2}

3.4. Normalization for mitochondrial content

Mitochondrial concentration, C_{mtE} , and mitochondrial markers

Mitochondria-specific flux, J_{mtE,O_2}

*3.5. Evaluation of mitochondrial markers**3.6. Conversion: units***4. Conclusions** – Box 3: Mitochondrial and cell respiration**5. References**

102 **Abstract** As the knowledge base and importance of mitochondrial physiology to human health
103 expand, the necessity for harmonizing nomenclature concerning mitochondrial respiratory
104 states and rates has become increasingly apparent. Clarity of concept and consistency of
105 nomenclature are key trademarks of a research field. These trademarks facilitate effective
106 transdisciplinary communication, education, and ultimately further discovery. Peter Mitchell's
107 chemiosmotic theory establishes the mechanism of energy transformation and coupling in
108 oxidative phosphorylation. The unifying concept of the protonmotive force provides the
109 framework for developing a consistent theory and nomenclature for mitochondrial physiology
110 and bioenergetics. Herein, we follow IUPAC guidelines on general terms of physical chemistry,
111 extended by considerations on open systems and irreversible thermodynamics. We align the
112 nomenclature and symbols of classical bioenergetics with a concept-driven constructive
113 terminology to express the meaning of each quantity clearly and consistently. In this position
114 statement, in the frame of COST Action MitoEAGLE, we endeavour to provide a balanced
115 view on mitochondrial respiratory control and a critical discussion on reporting data of
116 mitochondrial respiration in terms of metabolic flows and fluxes. Uniform standards for
117 evaluation of respiratory states and rates will ultimately support the development of databases
118 of mitochondrial respiratory function in species, tissues, and cells.

119

120 *Keywords:* Mitochondrial respiratory control, coupling control, mitochondrial
121 preparations, protonmotive force, oxidative phosphorylation, OXPHOS, efficiency, electron
122 transfer, ET; proton leak, LEAK, residual oxygen consumption, ROX, State 2, State 3, State 4,
123 normalization, flow, flux

124

125

126

127 **Executive summary**

128

129

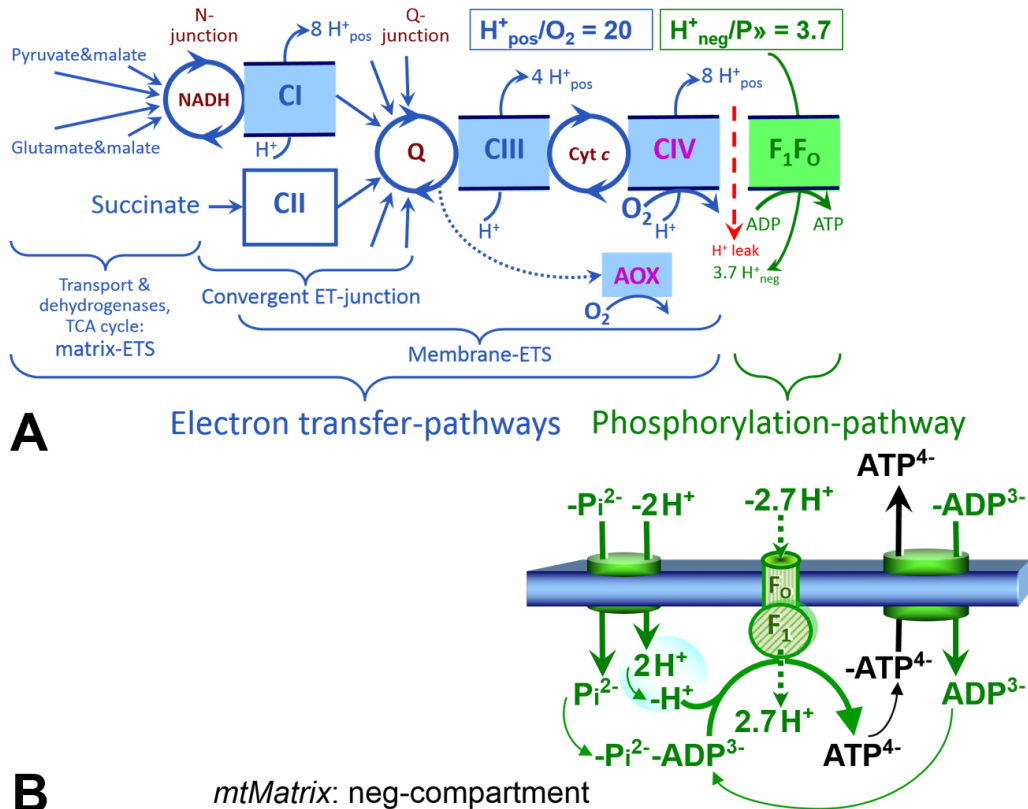
130 1. In view of broad implications on health care, mitochondrial researchers face an
131 increasing responsibility to disseminate their fundamental knowledge and novel
132 discoveries to a wide range of stakeholders and scientists beyond the group of
133 specialists. This requires implementation of a commonly accepted terminology
134 within the discipline and standardization in the translational context. Authors,
135 reviewers, journal editors, and lecturers are challenged to collaborate with the aim
136 to harmonize the nomenclature in the growing field of mitochondrial physiology
and bioenergetics.

137 2. Aerobic energy metabolism in mammalian mitochondria depends on the coupling of
138 ADP → ATP phosphorylation to oxygen consumption in catabolic reactions. In this
139 process of oxidative phosphorylation, coupling is mediated by translocation of
140 protons through respiratory proton pumps operating across the inner mitochondrial
141 membrane and generating or utilizing the protonmotive force measured between
142 the mitochondrial matrix and intermembrane compartment. Compartmental
143 coupling thus distinguishes vectorial oxidative phosphorylation from fermentation
144 as the counterpart of cellular core energy metabolism.

145 3. To exclude fermentation and other cytosolic interactions from exerting an effect on
146 mitochondrial metabolism, the barrier function of the plasma membrane must be
147 disrupted. Selective removal or permeabilization of the plasma membrane yields
148 mitochondrial preparations—including isolated mitochondria, tissue and cellular
149 preparations—with structural and functional integrity. Then extra-mitochondrial
150 concentrations of fuel substrates transported into the mitochondrial matrix, ADP,
151 ATP, inorganic phosphate, and cations including H⁺ can be controlled to determine
152 mitochondrial function under a set of conditions defined as coupling control states.

153
154
155
156
157

A concept-driven terminology of bioenergetics incorporates in its terms and symbols explicitly information on the nature of respiratory states, that makes the technical terms readily recognized and easy to understand.



158
159
160
161
162
163
164
165
166
167
168
169
170
171
172
173
174
175
176
177
178
179

Fig. 1. The oxidative phosphorylation (OXPHOS) system. (A) The mitochondrial electron transfer system (ETS) is fuelled by diffusion and transport of substrates across the mtOM and mtIM and consists of the matrix-ETS and membrane-ETS. ET-pathways are coupled to the phosphorylation-pathway. ET-pathways converge at the N-junction and Q-junction. Additional arrows indicate electron entry into the Q-junction through electron transferring flavoprotein, glycerophosphate dehydrogenase, dihydro-orotate dehydrogenase, choline dehydrogenase, and sulfide-ubiquinone oxidoreductase. The dotted arrow indicates the branched pathway of oxygen consumption by alternative quinol oxidase (AOX). The H^+_{pos}/O_2 ratio is the outward proton flux from the matrix space to the positively (pos) charged compartment, divided by catabolic O_2 flux in the NADH-pathway. The $H^+_{\text{neg}}/P \gg$ ratio is the inward proton flux from the inter-membrane space to the negatively (neg) charged matrix space, divided by the flux of phosphorylation of ADP to ATP (Eq. 1). These are not fixed stoichiometries due to ion leaks and proton slip. (B) Phosphorylation-pathway catalyzed by the proton pump F₁F₀-ATPase (F-ATPase), adenine nucleotide translocase, and inorganic phosphate transporter. The $H^+_{\text{neg}}/P \gg$ stoichiometry is the sum of the coupling stoichiometry in the F-ATPase reaction ($-2.7 H^+_{\text{pos}}$ from the positive intermembrane space, $2.7 H^+_{\text{neg}}$ to the matrix, *i.e.*, the negative compartment) and the proton balance in the translocation of ADP²⁻, ATP³⁻ and Pi²⁻. Modified from (A) Lemieux *et al.* (2017) and (B) Gnaiger (2014).

- 180 4. Mitochondrial coupling states are defined according to the control of respiratory oxygen
 181 consumption by the protonmotive force. Capacities of oxidative phosphorylation
 182 and electron transfer capacities are measured at kinetically saturating
 183 concentrations of fuel substrates, ADP and inorganic phosphate, or at optimal
 184 uncoupler concentrations, respectively. Respiratory capacities are a measure of the
 185 upper bound of the rates of respiration, providing reference values for the diagnosis
 186 of health and disease, and for evaluation of the effects of **E**volutionary background,
 187 **A**ge, **G**ender and sex, **L**ifestyle and **E**nvironment (EAGLE).
- 188 5. Some degree of uncoupling is a characteristic of energy-transformations across
 189 membranes. Uncoupling is caused by a variety of physiological, pathological,
 190 toxicological, pharmacological and environmental conditions that exert an
 191 influence not only on the proton leak and cation cycling, but also on proton slip
 192 within the proton pumps and the structural integrity of the mitochondria. A more
 193 loosely coupled state is induced by stimulation of mitochondrial superoxide
 194 formation and the bypass of proton pumps. In addition, uncoupling by application
 195 of protonophores represents an experimental intervention for the transition from a
 196 well-coupled to the noncoupled state of mitochondrial respiration.
- 197 6. Respiratory oxygen consumption rates have to be carefully normalized to enable meta-
 198 analytic studies beyond the specific question of a particular experiment. Therefore,
 199 all raw data should be published in a supplemental table or open access data
 200 repository. Normalization of rates for the volume of the experimental chamber (the
 201 measuring system) is distinguished from normalization for (1) the volume or mass
 202 of the experimental sample, (2) the number of objects (cells, organisms), and (3)
 203 the concentration of mitochondrial markers in the chamber.
- 204 7. The consistent use of terms and symbols discussed in this MitoEAGLE position
 205 statement will facilitate transdisciplinary communication and support further
 206 developments of a database on bioenergetics and mitochondrial physiology. The
 207 present considerations are focused on studies with mitochondrial preparations.
 208 These will be extended in a series of reports on pathway control of mitochondrial
 209 respiration, the protonmotive force, respiratory states in intact cells, and
 210 harmonization of experimental procedures.

215 **Box 1: In brief – Mitochondria and Bioblasts**

216 **Mitochondria** are the oxygen-consuming electrochemical generators evolved from
 217 endosymbiotic bacteria (Margulis 1970; Lane 2005). They were described by Richard Altmann
 218 (1894) as ‘bioblasts’, which include not only the mitochondria as presently defined, but also
 219 symbiotic and free-living bacteria. The word ‘mitochondria’ (Greek mitos: thread; chondros:
 220 granule) was introduced by Carl Benda (1898).

221 Mitochondrial dysfunction is associated with a wide variety of genetic and degenerative
 222 diseases. Robust mitochondrial function is supported by physical exercise and caloric balance,
 223 and is central for sustained metabolic health throughout life. Therefore, a more consistent
 224 presentation of mitochondrial physiology will improve our understanding of the etiology of
 225 disease, the diagnostic repertoire of mitochondrial medicine, with a focus on protective
 226 medicine, lifestyle and healthy aging.

227 We now recognize mitochondria as dynamic organelles with a double membrane that are
 228 contained within eukaryotic cells. The mitochondrial inner membrane (mtIM) shows dynamic
 229 tubular to disk-shaped cristae that separate the mitochondrial matrix, *i.e.*, the negatively charged
 230

231 internal mitochondrial compartment, and the intermembrane space; the latter being positively
232 charged and enclosed by the mitochondrial outer membrane (mtOM). The mtIM contains the
233 non-bilayer phospholipid cardiolipin, which is not present in any other eukaryotic cellular
234 membrane. Cardiolipin promotes the formation of respiratory supercomplexes, which are
235 supramolecular assemblies based upon specific, though dynamic, interactions between
236 individual respiratory complexes (Greggio *et al.* 2017; Lenaz *et al.* 2017). Membrane fluidity
237 exerts an influence on functional properties of proteins incorporated in the membranes
238 (Waczulikova *et al.* 2007).

239 Mitochondria are the structural and functional elements of cell respiration. Cell
240 respiration is the consumption of oxygen by electron transfer coupled to electrochemical proton
241 translocation across the mtIM. In the process of oxidative phosphorylation (OXPHOS), the
242 reduction of O₂ is electrochemically coupled to the transformation of energy in the form of
243 adenosine triphosphate (ATP; Mitchell 1961, 2011). Mitochondria are the powerhouses of the
244 cell which contain the machinery of the OXPHOS-pathways, including transmembrane
245 respiratory complexes—proton pumps with FMN, Fe-S and cytochrome *b*, *c*, *aa*₃ redox
246 systems); alternative dehydrogenases and oxidases; the coenzyme ubiquinone (Q); F-ATPase
247 or ATP synthase; the enzymes of the tricarboxylic acid cycle and fatty acid oxidation;
248 transporters of ions, metabolites and co-factors; and mitochondrial kinases related to energy
249 transfer pathways. The mitochondrial proteome comprises over 1,200 proteins (Calvo *et al.*
250 2015; 2017), mostly encoded by nuclear DNA (nDNA), with a variety of functions, many of
251 which are relatively well known (*e.g.*, apoptosis-regulating proteins), while others are still under
252 investigation, or need to be identified (*e.g.*, alanine transporter).

253 There is a constant crosstalk between mitochondria and the other cellular components.
254 The crosstalk between mitochondria and endoplasmic reticulum is involved in the regulation of
255 calcium homeostasis, cell division, autophagy, differentiation, anti-viral signaling (Murley and
256 Nunnari 2016). Cellular mitostasis is maintained through regulation at both the transcriptional
257 and post-translational level, through cell signalling including proteostatic (*e.g.*, the ubiquitin-
258 proteasome and autophagy-lysosome pathways), and genome stability modules throughout the
259 cell cycle or even cell death, contributing to homeostatic regulation in response to varying
260 energy demands and stress (Quiros *et al.* 2016). In addition to mitochondrial movement along
261 the microtubules, mitochondrial morphology can change in response to energy requirements of
262 the cell via processes known as fusion and fission, through which mitochondria communicate
263 within a network, and in response to intracellular stress factors causing swelling and ultimately
264 permeability transition.

265 Mitochondria typically maintain several copies of their own genome known as
266 mitochondrial DNA (mtDNA; hundred to thousands per cell; Cummins 1998), which is
267 maternally inherited. One exception to strictly maternal inheritance in animals is found in
268 bivalves (Breton *et al.* 2007; White *et al.* 2008). mtDNA is 16.5 kB in length, contains 13
269 protein-coding genes for subunits of the transmembrane respiratory Complexes CI, CIII, CIV
270 and F-ATPase, and also encodes 22 tRNAs and the mitochondrial 16S and 12S rRNA.
271 Additional gene content is encoded in the mitochondrial genome, *e.g.*, microRNAs, piRNA,
272 smithRNAs, repeat associated RNA, and even additional proteins (Duarte *et al.* 2014; Lee *et al.*
273 2015; Cobb *et al.* 2016). The mitochondrial genome is regulated and supplemented by
274 nuclear-encoded mitochondrial targeted proteins.

275 Abbreviation: mt, as generally used in mtDNA. Mitochondrion is singular and
276 mitochondria is plural.

277 *‘For the physiologist, mitochondria afforded the first opportunity for an experimental*
278 *approach to structure-function relationships, in particular those involved in active transport,*
279 *vectorial metabolism, and metabolic control mechanisms on a subcellular level’* (Ernster and
280 Schatz 1981).
281

282 1. Introduction

283

284 Mitochondria are the powerhouses of the cell with numerous physiological, molecular,
285 and genetic functions (**Box 1**). Every study of mitochondrial health and disease is faced with
286 **E**volution, **A**ge, **G**ender and sex, **L**ifestyle, and **E**nvironment (EAGLE) as essential background
287 conditions intrinsic to the individual patient or subject, cohort, species, tissue and to some extent
288 even cell line. As a large and coordinated group of laboratories and researchers, the mission of
289 the global MitoEAGLE Network is to generate the necessary scale, type, and quality of
290 consistent data sets and conditions to address this intrinsic complexity. Harmonization of
291 experimental protocols and implementation of a quality control and data management system
292 are required to interrelate results gathered across a spectrum of studies and to generate a
293 rigorously monitored database focused on mitochondrial respiratory function. In this way,
294 researchers within the same and across different disciplines will be positioned to compare
295 findings across traditions and generations to an agreed upon set of clearly defined and accepted
296 international standards.

297 Reliability and comparability of quantitative results depend on the accuracy of
298 measurements under strictly-defined conditions. A conceptual framework is required to warrant
299 meaningful interpretation and comparability of experimental outcomes carried out by research
300 groups at different institutes. With an emphasis on quality of research, collected data can be
301 useful far beyond the specific question of a particular experiment. Enabling meta-analytic
302 studies is the most economic way of providing robust answers to biological questions (Cooper
303 *et al.* 2009). Vague or ambiguous jargon can lead to confusion and may relegate valuable
304 signals to wasteful noise. For this reason, measured values must be expressed in standard units
305 for each parameter used to define mitochondrial respiratory function. Harmonization of
306 nomenclature and definition of technical terms are essential to improve the awareness of the
307 intricate meaning of current and past scientific vocabulary, for documentation and integration
308 into databases in general, and quantitative modelling in particular (Beard 2005). The focus on
309 coupling states and fluxes through metabolic pathways of aerobic energy transformation in
310 mitochondrial preparations is a first step in the attempt to generate a conceptually-oriented
311 nomenclature in bioenergetics and mitochondrial physiology. Coupling states of intact cells,
312 the protonmotive force, and respiratory control by fuel substrates and specific inhibitors of
313 respiratory enzymes will be reviewed in subsequent communications.

314

315

316 2. Oxidative phosphorylation and coupling states in mitochondrial preparations

317 *‘Every professional group develops its own technical jargon for talking about matters of*
318 *critical concern ... People who know a word can share that idea with other members of*
319 *their group, and a shared vocabulary is part of the glue that holds people together and*
320 *allows them to create a shared culture’ (Miller 1991).*

321

322 **Mitochondrial preparations** are defined as either isolated mitochondria, or tissue and
323 cellular preparations in which the barrier function of the plasma membrane is disrupted. Since
324 this entails the loss of cell viability, mitochondrial preparations are not studied *in vivo*. In
325 contrast to isolated mitochondria and tissue homogenate preparations, mitochondria in
326 permeabilized tissues and cells are *in situ* relative to the plasma membrane. The plasma
327 membrane separates the intracellular compartment including the cytosol, nucleus, and
328 organelles from the environment of the cell. The plasma membrane consists of a lipid bilayer,
329 embedded proteins, and attached organic molecules that collectively control the selective
330 permeability of ions, organic molecules, and particles across the cell boundary. The intact
331 plasma membrane prevents the passage of many water-soluble mitochondrial substrates and
332 inorganic ions—such as succinate, adenosine diphosphate (ADP) and inorganic phosphate (P_i),

333 that must be controlled at kinetically-saturating concentrations for the analysis of respiratory
334 capacities; this limits the scope of investigations into mitochondrial respiratory function in
335 intact cells.

336 The cholesterol content of the plasma membrane is high compared to mitochondrial
337 membranes. Therefore, mild detergents—such as digitonin and saponin—can be applied to
338 selectively permeabilize the plasma membrane by interaction with cholesterol and allow free
339 exchange of organic molecules and inorganic ions between the cytosol and the immediate cell
340 environment, while maintaining the integrity and localization of organelles, cytoskeleton, and
341 the nucleus. Application of optimum concentrations of permeabilization agents (mild detergents
342 or toxins) leads to the complete loss of cell viability, tested by nuclear staining and washout of
343 cytosolic marker enzymes—such as lactate dehydrogenase, while mitochondrial function
344 remains intact. The respiration rate of isolated mitochondria remains unaltered after the addition
345 of low concentrations of digitonin or saponin. In addition to mechanical permeabilization during
346 homogenization of tissue, permeabilization agents may be applied to ensure permeabilization
347 of all cells. Suspensions of cells permeabilized in the respiration chamber and crude tissue
348 homogenates contain all components of the cell at highly dilute concentrations. All
349 mitochondria are retained in chemically-permeabilized mitochondrial preparations and crude
350 tissue homogenates. In the preparation of isolated mitochondria, the cells or tissues are
351 homogenized, and the mitochondria are separated from other cell fractions and purified by
352 differential centrifugation, entailing the loss of a fraction of mitochondria. Typical
353 mitochondrial recovery ranges from 30% to 80%. Maximization of the purity of isolated
354 mitochondria may compromise not only the mitochondrial yield but also the structural and
355 functional integrity. Therefore, protocols to isolate mitochondria need to be optimized
356 according to each study. The term mitochondrial preparation does not include further
357 fractionation of mitochondrial components, neither submitochondrial particles.

358

359 *2.1. Respiratory control and coupling*

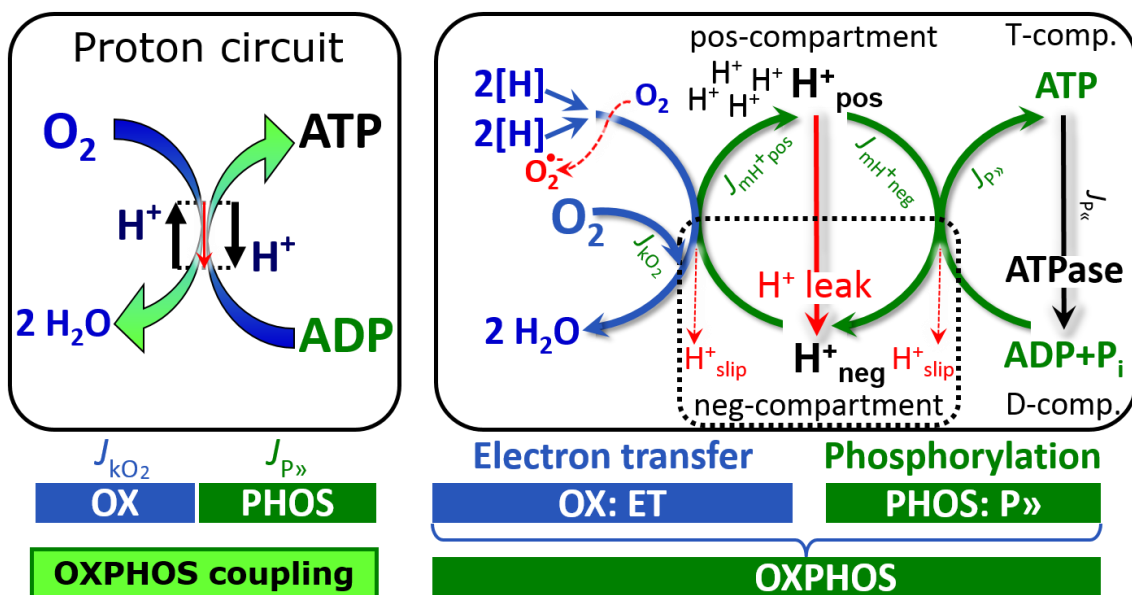
360

361 Respiratory coupling control states are established in studies of mitochondrial
362 preparations to obtain reference values for various output variables. Physiological conditions *in*
363 *vivo* deviate from these experimentally obtained states. Since kinetically-saturating
364 concentrations, *e.g.*, of ADP or oxygen, may not apply to physiological intracellular conditions,
365 relevant information is obtained in studies of kinetic responses to variations in [ADP] or [O₂]
366 in the range between kinetically-saturating concentrations and anoxia (Gnaiger 2001).

367 **The steady-state:** Mitochondria represent a thermodynamically open system in non-
368 equilibrium states of biochemical energy transformation. State variables (protonmotive force;
369 redox states) and metabolic *rates* (fluxes) are measured in defined mitochondrial respiratory
370 *states*. Steady-states can be obtained only in open systems, in which changes by *internal*
371 transformations, *e.g.*, O₂ consumption, are instantaneously compensated for by *external* fluxes,
372 *e.g.*, O₂ supply, preventing a change of oxygen concentration in the system (Gnaiger 1993b).
373 Mitochondrial respiratory states monitored in closed systems satisfy the criteria of pseudo-
374 steady states for limited periods of time, when changes in the system (concentrations of O₂, fuel
375 substrates, ADP, P_i, H⁺) do not exert significant effects on metabolic fluxes (respiration,
376 phosphorylation). Such pseudo-steady states require respiratory media with sufficient buffering
377 capacity and substrates maintained at kinetically-saturating concentrations, and thus depend on
378 the kinetics of the processes under investigation.

379 **Specification of biochemical dose:** Substrates, uncouplers, inhibitors, and other
380 biochemical reagents are titrated to dissect mitochondrial function. Nominal concentrations of
381 these substances are usually reported as initial amount of substance concentration [mol·L⁻¹] in
382 the incubation medium. When aiming at the measurement of kinetically saturated processes—
383 such as OXPHOS-capacities, the concentrations for substrates can be chosen according to the

384 apparent equilibrium constant, K_m' . In the case of hyperbolic kinetics, only 80% of maximum
 385 respiratory capacity is obtained at a substrate concentration of four times the K_m' , whereas
 386 substrate concentrations of 5, 9, 19 and 49 times the K_m' are theoretically required for reaching
 387 83%, 90%, 95% or 98% of the maximal rate (Gnaiger 2001). Other reagents are chosen to
 388 inhibit or alter some process. The amount of these chemicals in an experimental incubation is
 389 selected to maximize effect, yet not lead to unacceptable off-target consequences that would
 390 adversely affect the data being sought. Specifying the amount of substance in an incubation as
 391 nominal concentration in the aqueous incubation medium can be ambiguous (Doskey *et al.*
 392 2015), particularly when lipophilic substances (oligomycin; uncouplers, permeabilization
 393 agents) or cations (TPP⁺; fluorescent dyes such as safranin, TMRM) are applied which
 394 accumulate in biological membranes or the mitochondrial matrix. For example, a dose of
 395 digitonin of 8 fmol·cell⁻¹ (10 pg·cell⁻¹; 10 μg·10⁻⁶ cells) is optimal for permeabilization of
 396 endothelial cells, and the concentration in the incubation medium has to be adjusted according
 397 to the cell density applied (Doerrier *et al.* 2018). Generally, dose/exposure can be specified per
 398 unit of biological sample, *i.e.*, (nominal moles of xenobiotic)/(number of cells) [mol·cell⁻¹] or,
 399 as appropriate, per mass of biological sample [mol·kg⁻¹]. This approach to specification of
 400 dose/exposure provides a scalable parameter that can be used to design experiments, help
 401 interpret a wide variety of experimental results, and provide absolute information that allows
 402 researchers worldwide to make the most use of published data (Doskey *et al.* 2015).
 403



404
 405 **Fig. 2. The proton circuit and coupling in oxidative phosphorylation (OXPHOS).** 2[H]
 406 indicates the reduced hydrogen equivalents of fuel substrates of the catabolic reaction k with
 407 oxygen. Oxygen flux, J_{kO_2} , through the catabolic ET-pathway, is coupled to flux through the
 408 phosphorylation-pathway of ADP to ATP, $J_{P\gg}$. The proton pumps of the ET-pathway drive
 409 proton flux into the positive (pos) compartment, J_{mH^+pos} , generating the output protonmotive
 410 force (motive, subscript m). F-ATPase is coupled to inward proton current into the negative
 411 (neg) compartment, J_{mH^+neg} , to phosphorylate ADP+P_i to ATP. The system defined by the
 412 boundaries (full black line) is not a black box, but is analysed as a compartmental system. The
 413 negative compartment (neg-compartment, enclosed by the dotted line) is the matrix space,
 414 separated by the mtIM from the positive compartment (pos-compartment). ADP+P_i and ATP
 415 are the substrate- and product-compartments (scalar ADP and ATP compartments, D-comp.
 416 and T-comp.), respectively. At steady-state proton turnover, $J_{\infty H^+}$, and ATP turnover, $J_{\infty P}$,
 417 maintain concentrations constant, when $J_{mH^+\infty} = J_{mH^+pos} = J_{mH^+neg}$, and $J_{P\infty} = J_{P\gg} = J_{P\ll}$. Modified
 418 from Gnaiger (2014).

419 **Phosphorylation, P \gg , and P \gg /O $_2$ ratio:** *Phosphorylation* in the context of OXPHOS is
 420 defined as phosphorylation of ADP by P $_i$ to ATP. On the other hand, the term phosphorylation
 421 is used generally in many contexts, *e.g.*, protein phosphorylation. This justifies consideration
 422 of a symbol more discriminating and specific than P as used in the P/O ratio (phosphate to
 423 atomic oxygen ratio), where P indicates phosphorylation of ADP to ATP or GDP to GTP. We
 424 propose the symbol P \gg for the endergonic (uphill) direction of phosphorylation ADP \rightarrow ATP,
 425 and likewise the symbol P \ll for the corresponding exergonic (downhill) hydrolysis ATP \rightarrow ADP
 426 (**Fig. 2**). P \gg refers mainly to electrontransfer phosphorylation but may also involve substrate-
 427 level phosphorylation as part of the tricarboxylic acid (TCA) cycle (succinyl-CoA ligase) and
 428 phosphorylation of ADP catalyzed by phosphoenolpyruvate carboxykinase.
 429 Transphosphorylation is performed by adenylate kinase, creatine kinase, hexokinase and
 430 nucleoside diphosphate kinase. In isolated mammalian mitochondria, ATP production
 431 catalyzed by adenylate kinase (2 ADP \leftrightarrow ATP + AMP) proceeds without fuel substrates in the
 432 presence of ADP (Komlódi and Tretter 2017). Kinase cycles are involved in intracellular energy
 433 transfer and signal transduction for regulation of energy flux.

434 The P \gg /O $_2$ ratio (P \gg /4 e $^-$) is two times the ‘P/O’ ratio (P \gg /2 e $^-$) of classical bioenergetics.
 435 P \gg /O $_2$ is a generalized symbol, independent phosphorylation assessment by determination of P $_i$
 436 consumption (P $_i$ /O $_2$ flux ratio), ADP depletion (ADP/O $_2$ flux ratio), or ATP production
 437 (ATP/O $_2$ flux ratio). The mechanistic P \gg /O $_2$ ratio—or P \gg /O $_2$ stoichiometry—is calculated from
 438 the proton-to-oxygen and proton-to-phosphorylation coupling stoichiometries (**Fig. 1A**),
 439

$$440 \quad P\gg/O_2 = \frac{H_{\text{pos}}^+/O_2}{H_{\text{neg}}^+/P\gg} \quad (1)$$

441
 442 The H $^+$ _{pos}/O $_2$ *coupling stoichiometry* (referring to the full 4 electron reduction of O $_2$) depends
 443 on the ET-pathway control state which defines the relative involvement of the three coupling
 444 sites (CI, CIII and CIV) in the catabolic pathway of electrons to O $_2$. This varies with: (1) a
 445 bypass of CI by single or multiple electron input into the Q-junction; and (2) a bypass of CIV
 446 by involvement of AOX. H $^+$ _{pos}/O $_2$ is 12 in the ET-pathways involving CIII and CIV as proton
 447 pumps, increasing to 20 for the NADH-pathway (**Fig. 1A**), but a general consensus on H $^+$ _{pos}/O $_2$
 448 stoichiometries remains to be reached (Hinkle 2005; Wikström and Hummer 2012; Sazanov
 449 2015). The H $^+$ _{neg}/P \gg coupling stoichiometry (3.7; **Fig. 1A**) is the sum of 2.7 H $^+$ _{neg} required by
 450 the F-ATPase of vertebrate and most invertebrate species (Watt *et al.* 2010) and the proton
 451 balance in the translocation of ADP, ATP and P $_i$ (**Fig. 1B**). Taken together, the mechanistic
 452 P \gg /O $_2$ ratio is calculated at 5.4 and 3.3 for NADH- and succinate-linked respiration, respectively
 453 (Eq. 1). The corresponding classical P \gg /O ratios (referring to the 2 electron reduction of 0.5 O $_2$)
 454 are 2.7 and 1.6 (Watt *et al.* 2010), in agreement with the measured P \gg /O ratio for succinate of
 455 1.58 \pm 0.02 (Gnaiger *et al.* 2000).

456 The effective P \gg /O $_2$ flux ratio ($Y_{P\gg/O_2} = J_{P\gg}/J_{kO_2}$) is diminished relative to the mechanistic
 457 P \gg /O $_2$ ratio by intrinsic and extrinsic uncoupling and dyscoupling (**Fig. 3**). Such generalized
 458 uncoupling is different from switching to mitochondrial pathways that involve fewer than three
 459 proton pumps (‘coupling sites’: Complexes CI, CIII and CIV), bypassing CI through multiple
 460 electron entries into the Q-junction, or CIII and CIV through AOX (**Fig. 1**). Reprogramming of
 461 mitochondrial pathways may be considered as a switch of gears (changing the stoichiometry)
 462 rather than uncoupling (loosening the stoichiometry). In addition, $Y_{P\gg/O_2}$ depends on several
 463 experimental conditions of flux control, increasing as a hyperbolic function of [ADP] to a
 464 maximum value (Gnaiger 2001).

465 **Control and regulation:** The terms metabolic *control* and *regulation* are frequently used
 466 synonymously, but are distinguished in metabolic control analysis: ‘We could understand the
 467 regulation as the mechanism that occurs when a system maintains some variable constant over
 468 time, in spite of fluctuations in external conditions (homeostasis of the internal state). On the

469 other hand, metabolic control is the power to change the state of the metabolism in response to
 470 an external signal' (Fell 1997). Respiratory control may be induced by experimental control
 471 signals that *exert* an influence on: (1) ATP demand and ADP phosphorylation-rate; (2) fuel
 472 substrate composition, pathway competition; (3) available amounts of substrates and oxygen,
 473 *e.g.*, starvation and hypoxia; (4) the protonmotive force, redox states, flux–force relationships,
 474 coupling and efficiency; (5) Ca²⁺ and other ions including H⁺; (6) inhibitors, *e.g.*, nitric oxide
 475 or intermediary metabolites such as oxaloacetate; (7) signalling pathways and regulatory
 476 proteins, *e.g.*, insulin resistance, transcription factor hypoxia inducible factor 1. *Mechanisms* of
 477 respiratory control and regulation include adjustments of: (1) enzyme activities by allosteric
 478 mechanisms and phosphorylation; (2) enzyme content, concentrations of cofactors and
 479 conserved moieties—such as adenylates, nicotinamide adenine dinucleotide [NAD⁺/NADH],
 480 coenzyme Q, cytochrome *c*); (3) metabolic channeling by supercomplexes; and (4)
 481 mitochondrial density (enzyme concentrations and membrane area) and morphology (cristae
 482 folding, fission and fusion). Mitochondria are targeted directly by hormones, thereby affecting
 483 their energy metabolism (Lee *et al.* 2013; Gerö and Szabo 2016; Price and Dai 2016; Moreno
 484 *et al.* 2017). Evolutionary or acquired differences in the genetic and epigenetic basis of
 485 mitochondrial function (or dysfunction) between subjects and gene therapy; age; gender,
 486 biological sex, and hormone concentrations; life style including exercise and nutrition; and
 487 environmental issues including thermal, atmospheric, toxicological and pharmacological
 488 factors, exert an influence on all control mechanisms listed above. For reviews, see Brown
 489 1992; Gnaiger 1993a, 2009; 2014; Paradies *et al.* 2014; Morrow *et al.* 2017.

490 **Respiratory control and response:** Lack of control by a metabolic pathway, *e.g.*,
 491 phosphorylation-pathway, means that there will be no response to a variable activating it, *e.g.*,
 492 [ADP]. The reverse, however, is not true as the absence of a response to [ADP] does not exclude
 493 the phosphorylation-pathway from having some degree of control. The degree of control of a
 494 component of the OXPHOS-pathway on an output variable—such as oxygen flux, will in
 495 general be different from the degree of control on other outputs—such as phosphorylation-flux
 496 or proton leak flux. Therefore, it is necessary to be specific as to which input and output are
 497 under consideration (Fell 1997).

498 **Respiratory coupling control and ET-pathway control:** Respiratory control refers to
 499 the ability of mitochondria to adjust oxygen consumption in response to external control signals
 500 by engaging various mechanisms of control and regulation. Respiratory control is monitored in
 501 a mitochondrial preparation under conditions defined as respiratory states. When
 502 phosphorylation of ADP to ATP is stimulated or depressed, an increase or decrease is observed
 503 in electron flux linked to oxygen consumption in respiratory coupling states of intact
 504 mitochondria ('controlled states' in the classical terminology of bioenergetics). Alternatively,
 505 coupling of electron transfer with phosphorylation is disengaged by disruption of the integrity
 506 of the mtIM or by uncouplers, functioning like a clutch in a mechanical system. The
 507 corresponding coupling control state is characterized by high levels of oxygen consumption
 508 without control by P» ('uncontrolled state').

509 ET-pathway control states are obtained in mitochondrial preparations by depletion of
 510 endogenous substrates and addition to the mitochondrial respiration medium of fuel substrates
 511 (CHNO; 2[H] in **Fig. 2**) and specific inhibitors, activating selected mitochondrial catabolic
 512 pathways, *k* (**Fig. 1**). Coupling control states and pathway control states are complementary,
 513 since mitochondrial preparations depend on an exogenous supply of pathway-specific fuel
 514 substrates and oxygen (Gnaiger 2014).

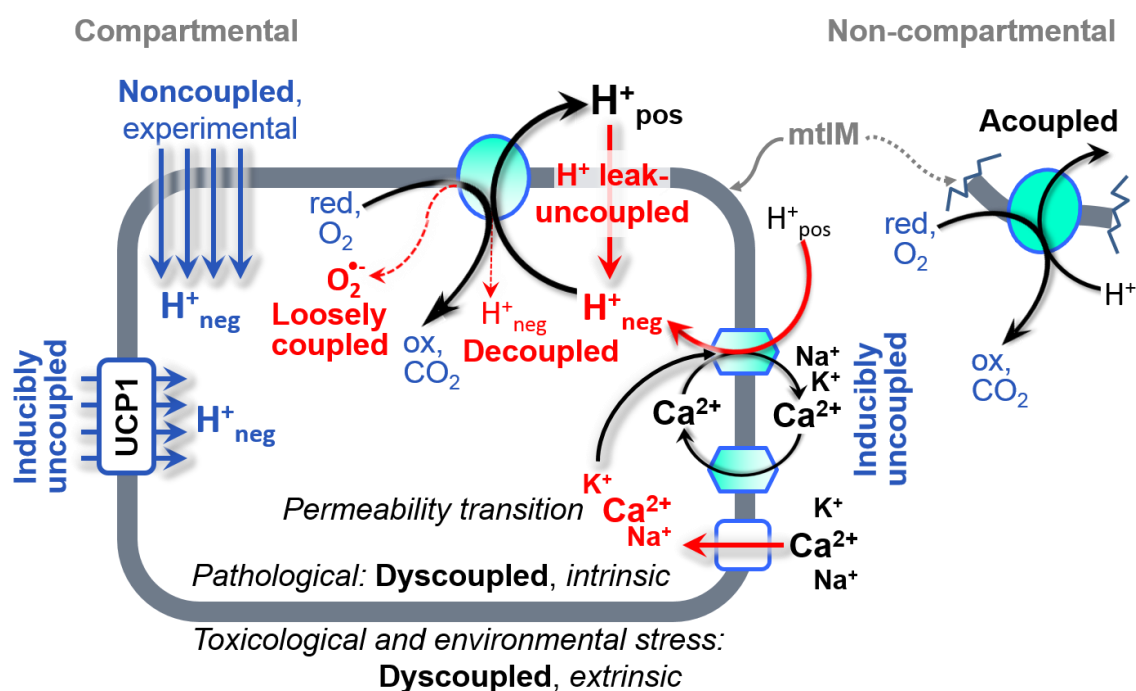
515 **Coupling:** In mitochondrial electron transfer (**Fig. 1**), vectorial transmembrane proton
 516 flux is coupled through the proton pumps CI, CIII and CIV to the catabolic flux of scalar
 517 reactions, collectively measured as oxygen flux (**Fig. 2**). Thus mitochondria are elements of
 518 energy transformation. Energy cannot be lost or produced in any internal process (First Law of
 519 thermodynamics). Open and closed systems can gain or loose energy only by external fluxes—

520 by exchange with the environment. Energy is a conserved quantity. Therefore, energy can
 521 neither be produced by mitochondria, nor is there any internal process without energy
 522 conservation. Exergy is defined as the ‘free energy’ with the potential to perform work.
 523 *Coupling* is the mechanistic linkage of an exergonic process (spontaneous, negative exergy
 524 change) with an endergonic process (positive exergy change) in energy transformations which
 525 conserve part of the exergy that would be irreversible lost or dissipated in an uncoupled process.

526 **Uncoupling:** Uncoupling of mitochondrial respiration is a general term comprising
 527 diverse mechanisms. Differences of terms—uncoupled *vs.* noncoupled—are easily overlooked,
 528 although they relate to different mechanisms of uncoupling (**Fig. 3**).

- 529 1. Proton leak across the mtIM from the pos- to the neg-compartment (**Fig. 2**);
- 530 2. Cycling of other cations, strongly stimulated by permeability transition;
- 531 3. Proton slip in the proton pumps when protons are effectively not pumped (CI, CIII and
 532 CIV) or are not driving phosphorylation (F-ATPase);
- 533 4. Loss of compartmental integrity when electron transfer is acoupled;
- 534 5. Electron leak in the loosely coupled univalent reduction of oxygen (O_2 ; dioxygen) to
 535 superoxide ($O_2^{\bullet -}$; superoxide anion radical).

536



537 **Fig 3. Mechanisms of respiratory uncoupling.** An intact mitochondrial inner membrane,
 538 mtIM, is required for vectorial, compartmental coupling. ‘Acoupled’ respiration is the
 539 consequence of structural disruption with catalytic activity of non-compartmental
 540 mitochondrial fragments. Inducibly uncoupled (activation of UCP1) and experimentally
 541 noncoupled respiration (titration of protonophores) stimulate respiration to maximum oxygen
 542 flux. H^+ leak-uncoupled, decoupled, and loosely coupled respiration are components of intrinsic
 543 uncoupling. Pathological dysfunction may affect all types of uncoupling, including
 544 permeability transition, causing intrinsically dyscoupled respiration. Similarly, toxicological
 545 and environmental stress factors can cause extrinsically dyscoupled respiration.

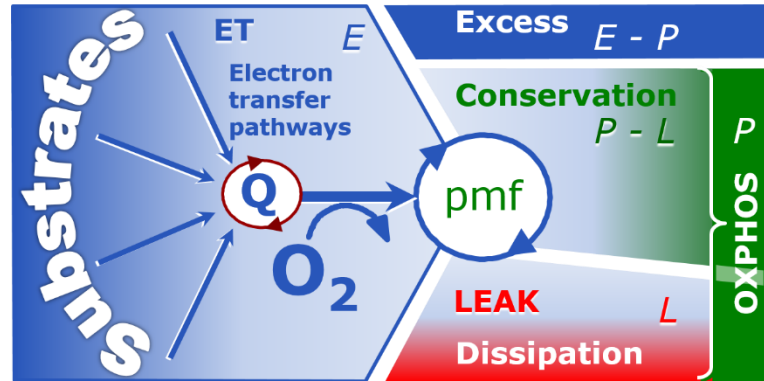
548 2.2. Coupling states and respiratory rates

549
 550 **Respiratory capacities in coupling control states:** To extend the classical nomenclature
 551 on mitochondrial coupling states (Section 2.3) by a concept-driven terminology that
 552 incorporates explicitly information on the nature of respiratory states, the terminology must be

553 general and not restricted to any particular experimental protocol or mitochondrial preparation
 554 (Gnaiger 2009). We focus primarily on the conceptual ‘why’, along with clarification of the
 555 experimental ‘how’. Respiratory capacities delineate, comparable to channel capacity in
 556 information theory (Schneider 2006), the upper bound of the rate of respiration measured in
 557 defined coupling control states and electron transfer-pathway (ET-pathway) states (Fig. 4).
 558

559 **Fig. 4. Four-compartment**
 560 **model of oxidative**

561 **phosphorylation.** Respiratory
 562 states (ET, OXPHOS, LEAK;
 563 **Table 1**) and corresponding rates
 564 (E , P , L) are connected by the
 565 protonmotive force, pmf. ET-
 566 capacity, E , is partitioned into (1)
 567 dissipative LEAK-respiration, L ,
 568 when the Gibbs energy change of
 569 catabolic O_2 consumption is



570 irreversibly lost, (2) net OXPHOS-capacity, $P-L$, with partial conservation of the capacity to
 571 perform work, and (3) the excess capacity, $E-P$. Modified from Gnaiger (2014).
 572

573 **Table 1. Coupling states and residual oxygen consumption in mitochondrial**
 574 **preparations in relation to respiration- and phosphorylation-rate, J_{kO_2} and $J_{P_{\gg}}$,**
 575 **and protonmotive force, Δp .** Coupling states are established at kinetically-saturating
 576 concentrations of fuel substrates and O_2 .

State	J_{kO_2}	$J_{P_{\gg}}$	Δp	Inducing factors	Limiting factors
LEAK	L ; low, cation leak-dependent respiration	0	max.	proton leak, slip, and cation cycling	$J_{P_{\gg}} = 0$: (1) without ADP, L_N ; (2) max. ATP/ADP ratio, L_T ; or (3) inhibition of the phosphorylation-pathway, L_{Omy}
OXPHOS	P ; high, ADP-stimulated respiration	max.	high	kinetically-saturating [ADP] and $[P_i]$	$J_{P_{\gg}}$, by phosphorylation-pathway; or J_{kO_2} by ET-capacity
ET	E ; max., noncoupled respiration	0	low	optimal external uncoupler concentration for max. $J_{O_2, E}$	J_{kO_2} by ET-capacity
ROX	R_{ox} ; min., residual O_2 consumption	0	0	$J_{O_2, Rox}$ in non-ET-pathway oxidation reactions	full inhibition of ET-pathway; or absence of fuel substrates

577
 578 To provide a diagnostic reference for respiratory capacities of core energy metabolism,
 579 the capacity of *oxidative phosphorylation*, OXPHOS, is measured at kinetically-saturating
 580 concentrations of ADP and P_i . The *oxidative* ET-capacity reveals the limitation of OXPHOS-
 581 capacity mediated by the *phosphorylation*-pathway. The ET- and phosphorylation-pathways
 582 comprise coupled segments of the OXPHOS-system. ET-capacity is measured as noncoupled
 583 respiration by application of *external uncouplers*. The contribution of *intrinsically uncoupled*

584 oxygen consumption is studied in the absence of ADP—by not stimulating phosphorylation, or
 585 by inhibition of the phosphorylation-pathway. The corresponding states are collectively
 586 classified as LEAK-states, when oxygen consumption compensates mainly for ion leaks,
 587 including the proton leak. Defined coupling states are induced by: (1) adding cation chelators
 588 such as EGTA, binding free Ca^{2+} and thus limiting cation cycling; (2) adding ADP and P_i ; (3)
 589 inhibiting the phosphorylation-pathway; and (4) uncoupler titrations, while maintaining a
 590 defined ET-pathway state with constant fuel substrates and inhibitors of specific branches of
 591 the ET-pathway (**Fig. 1**).

592 The three coupling states, ET, LEAK and OXPHOS, are shown schematically with the
 593 corresponding respiratory rates, abbreviated as E , L and P , respectively (**Fig. 4**). We distinguish
 594 metabolic *pathways* from metabolic *states* and the corresponding metabolic *rates*; for example:
 595 ET-pathways (**Fig. 4**), ET-state (**Fig. 5C**), and ET-capacity, E , respectively (**Table 1**). The
 596 protonmotive force is *high* in the OXPHOS-state when it drives phosphorylation, *maximum* in
 597 the LEAK-state of coupled mitochondria, driven by LEAK-respiration at a minimum back flux
 598 of cations to the matrix side, and *very low* in the ET-state when uncouplers short-circuit the
 599 proton cycle (**Table 1**).

600 E may exceed or be equal to P . $E > P$ is observed in many types of mitochondria, varying
 601 between species, tissues and cell types (Gnaiger 2009). $E - P$ is the excess ET-capacity pushing
 602 the phosphorylation-flux (**Fig. 1B**) to the limit of its *capacity of utilizing* the protonmotive force.
 603 In addition, the magnitude of $E - P$ depends on the tightness of respiratory coupling or degree of
 604 uncoupling, since an increase of L causes P to increase towards the limit of E . The *excess* $E - P$
 605 capacity, $E - P$, therefore, provides a sensitive diagnostic indicator of specific injuries of the
 606 phosphorylation-pathway, under conditions when E remains constant but P declines relative to
 607 controls (**Fig. 4**). Substrate cocktails supporting simultaneous convergent electron transfer to
 608 the Q-junction for reconstitution of TCA cycle function establish pathway control states with
 609 high ET-capacity, and consequently increase the sensitivity of the $E - P$ assay.

610 E cannot theoretically be lower than P . $E < P$ must be discounted as an artefact, which
 611 may be caused experimentally by: (1) loss of oxidative capacity during the time course of the
 612 respirometric assay, since E is measured subsequently to P ; (2) using insufficient uncoupler
 613 concentrations; (3) using high uncoupler concentrations which inhibit ET (Gnaiger 2008); (4)
 614 high oligomycin concentrations applied for measurement of L before titrations of uncoupler,
 615 when oligomycin exerts an inhibitory effect on E . On the other hand, the excess ET-capacity is
 616 overestimated if non-saturating $[\text{ADP}]$ or $[\text{P}_i]$ are used. See State 3 in the next section.

617 The net OXPHOS-capacity is calculated by subtracting L from P (**Fig. 4**). Then the net
 618 $P \gg \text{O}_2$ equals $P \gg / (P - L)$, wherein the dissipative LEAK component in the OXPHOS-state may
 619 be overestimated. This can be avoided by measuring LEAK-respiration in a state when the
 620 protonmotive force is adjusted to its slightly lower value in the OXPHOS-state—by titration of
 621 an ET inhibitor (Divakaruni and Brand 2011). Any turnover-dependent components of proton
 622 leak and slip, however, are underestimated under these conditions (Garlid *et al.* 1993). In
 623 general, it is inappropriate to use the term *ATP production* or *ATP turnover* for the difference
 624 of oxygen consumption measured in states P and L . The difference $P - L$ is the upper limit of the
 625 part of OXPHOS-capacity that is freely available for ATP production (corrected for LEAK-
 626 respiration) and is fully coupled to phosphorylation with a maximum mechanistic stoichiometry
 627 (**Fig. 4**).

628 **LEAK-state (Fig. 5A):** The LEAK-state is defined as a state of mitochondrial respiration
 629 when O_2 flux mainly compensates for ion leaks in the absence of ATP synthesis, at kinetically-
 630 saturating concentrations of O_2 and respiratory fuel substrates. LEAK-respiration is measured
 631 to obtain an estimate of *intrinsic uncoupling* without addition of an experimental uncoupler: (1)

632 in the absence of adenylates; (2)
 633 after depletion of ADP at a
 634 maximum ATP/ADP ratio; or (3)
 635 after inhibition of the
 636 phosphorylation-pathway
 637 by inhibitors of F-ATPase—such as
 638 oligomycin, or of adenine
 639 nucleotide translocase—such as
 640 carboxyatractyloside.

641 Adjustment of the nominal
 642 concentration of these inhibitors
 643 to the density of biological
 644 sample applied can minimize or
 645 avoid inhibitory side-effects
 646 exerted on ET-capacity or even
 647 some dyscoupling.

648 **Proton leak and**
 649 **uncoupled respiration:** Proton
 650 leak is a leak current of protons.
 651 The intrinsic proton leak is the
 652 *uncoupled* process in which
 653 protons diffuse across the mtIM
 654 in the dissipative direction of the
 655 downhill protonmotive force
 656 without coupling to
 657 phosphorylation (Fig. 5A). The
 658 proton leak flux depends non-
 659 linearly on the protonmotive
 660 force (Garlid *et al.* 1989;
 661 Divakaruni and Brand 2011), it is
 662 a property of the mtIM and may
 663 be enhanced due to possible
 664 contaminations by free fatty
 665 acids. Inducible uncoupling
 666 mediated by uncoupling protein
 667 1 (UCP1) is physiologically
 668 controlled, *e.g.*, in brown
 669 adipose tissue. UCP1 is a
 670 member of the mitochondrial
 671 carrier family which is involved
 672 in the translocation of protons
 673 across the mtIM (Klingenberg
 674 2017). Consequently, the short-
 675 circuit diminishes the protonmotive
 676 force and stimulates electron transfer to O₂ and heat
 677 dissipation without phosphorylation of ADP.

677 **Cation cycling:** There can be other cation contributors to leak current including calcium
 678 and probably magnesium. Calcium current is balanced by mitochondrial Na⁺/Ca²⁺ exchange,
 679 which is balanced by Na⁺/H⁺ or K⁺/H⁺ exchanges. This is another effective uncoupling
 680 mechanism different from proton leak.

681
 682

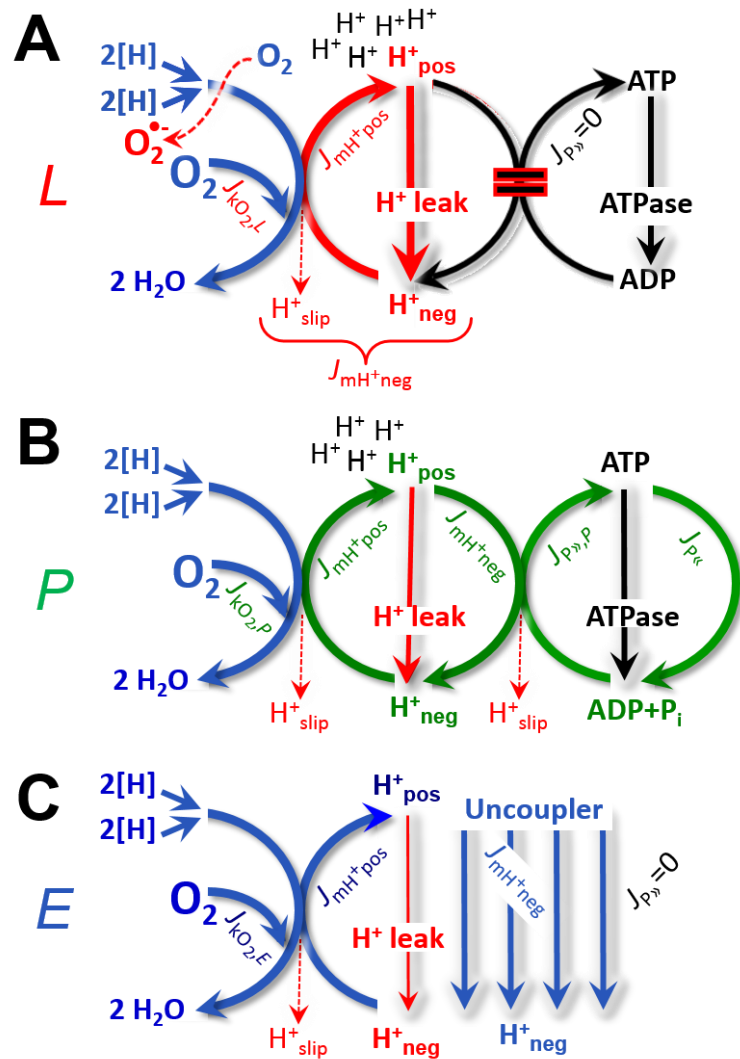


Fig. 5. Respiratory coupling states. A: LEAK-state and rate, L: Phosphorylation is arrested, $J_{P>} = 0$, and catabolic oxygen flux, $J_{kO_2,L}$, is controlled mainly by the proton leak, $J_{mH^{+}neg,L}$, at maximum protonmotive force (Fig. 3). **B: OXPHOS-state and rate, P:** Phosphorylation, $J_{P>}$, is stimulated by kinetically-saturating [ADP] and [P_i], and is supported by a high protonmotive force. O₂ flux, $J_{kO_2,P}$, is well-coupled at a $P>/O_2$ ratio of $J_{P>,P}/J_{O_2,P}$. **C: ET-state and rate, E:** Noncoupled respiration, $J_{kO_2,E}$, is maximum at optimum exogenous uncoupler concentration and phosphorylation is zero, $J_{P>} = 0$. See also Fig. 2.

683 **Table 2. Terms on respiratory coupling and uncoupling.**

Term	$J_{\text{K}O_2}$	P_{\gg}/O_2	Note	
acoupled		0	electron transfer in mitochondrial fragments without vectorial proton translocation (Fig. 3)	
intrinsic, no protonophore added	uncoupled	L	0	non-phosphorylating LEAK-respiration (Fig. 5A)
	proton leak-uncoupled		0	component of L , H^+ diffusion across the mtIM (Fig. 3)
	decoupled		0	component of L , proton slip (Fig. 3)
	loosely coupled		0	component of L , lower coupling due to superoxide formation and bypass of proton pumps (Fig. 3)
	dyscoupled		0	pathologically, toxicologically, environmentally increased uncoupling, mitochondrial dysfunction
	inducibly uncoupled		0	by UCP1 or cation (<i>e.g.</i> , Ca^{2+}) cycling (Fig. 3)
noncoupled	E	0	non-phosphorylating respiration stimulated to maximum flux at optimum exogenous uncoupler concentration (Fig. 5C)	
well-coupled	P	high	phosphorylating respiration with an intrinsic LEAK component (Fig. 5B)	
fully coupled	$P - L$	max.	OXPPOS-capacity corrected for LEAK-respiration (Fig. 4)	

684
685 **Proton slip and decoupled respiration:** Proton slip is the *decoupled* process in which
686 protons are only partially translocated by a proton pump of the ET-pathways and slip back to
687 the original compartment. The proton leak is the dominant contributor to the overall leak current
688 in mammalian mitochondria incubated under physiological conditions at 37 °C, whereas proton
689 slip is increased at lower experimental temperature (Canton *et al.* 1995). Proton slip can also
690 happen in association with the F-ATPase, in which the proton slips downhill across the pump
691 to the matrix without contributing to ATP synthesis. In each case, proton slip is a property of
692 the proton pump and increases with the pump turnover rate.

693 **Electron leak and loosely coupled respiration:** Superoxide production by the ETS leads
694 to a bypass of proton pumps and correspondingly lower P_{\gg}/O_2 ratio. This depends on the actual
695 site of electron leak and the scavenging of hydrogen peroxide by cytochrome *c*, whereby
696 electrons may re-enter the ETS with proton translocation by CIV.

697 **Loss of compartmental integrity and acoupled respiration:** Electron transfer and O_2
698 consumption proceed without compartmental proton translocation in disrupted mitochondrial
699 fragments. Such fragments form during mitochondrial isolation, and may not fully fuse to re-
700 establish structurally intact mitochondria. Loss of mtIM integrity, therefore, is the cause of
701 acoupled respiration, which is a nonvectorial dissipative process without control by the
702 protonmotive force.

703 **Dyscoupled respiration:** Mitochondrial injuries may lead to *dyscoupling* as a
704 pathological or toxicological cause of *uncoupled* respiration. Dyscoupling may involve any
705 type of uncoupling mechanism, *e.g.*, opening the permeability transition pore. Dyscoupled
706 respiration is distinguished from the experimentally induced *noncoupled* respiration in the ET-
707 state (**Fig. 3**).

708 **OXPPOS-state (Fig. 5B):** The OXPPOS-state is defined as the respiratory state with
709 kinetically-saturating concentrations of O_2 , respiratory and phosphorylation substrates, and

710 absence of exogenous uncoupler, which provides an estimate of the maximal respiratory
 711 capacity in the OXPHOS-state for any given ET-pathway state. Respiratory capacities at
 712 kinetically-saturating substrate concentrations provide reference values or upper limits of
 713 performance, aiming at the generation of data sets for comparative purposes. Physiological
 714 activities and effects of substrate kinetics can be evaluated relative to the OXPHOS-capacity.

715 As discussed previously, 0.2 mM ADP does not fully saturate flux in isolated
 716 mitochondria (Gnaiger 2001; Puchowicz *et al.* 2004); greater ADP concentration is required,
 717 particularly in permeabilized muscle fibres and cardiomyocytes, to overcome limitations by
 718 intracellular diffusion and by the reduced conductance of the mtOM (Jepihhina *et al.* 2011,
 719 Illaste *et al.* 2012, Simson *et al.* 2016), either through interaction with tubulin (Rostovtseva *et*
 720 *al.* 2008) or other intracellular structures (Birkedal *et al.* 2014). In permeabilized muscle fibre
 721 bundles of high respiratory capacity, the apparent K_m for ADP increases up to 0.5 mM (Saks *et*
 722 *al.* 1998), consistent with experimental evidence that >90% saturation is reached only at >5
 723 mM ADP (Pesta and Gnaiger 2012). Similar ADP concentrations are also required for accurate
 724 determination of OXPHOS-capacity in human clinical cancer samples and permeabilized cells
 725 (Klepinin *et al.* 2016; Koit *et al.* 2017). Whereas 2.5 to 5 mM ADP is sufficient to obtain the
 726 actual OXPHOS-capacity in many types of permeabilized tissue and cell preparations,
 727 experimental validation is required in each specific case.

728 **Electron transfer-state (Fig. 5C):** The ET-state is defined as the *noncoupled* state with
 729 kinetically-saturating concentrations of O₂, respiratory substrate and optimum *exogenous*
 730 uncoupler concentration for maximum O₂ flux, as an estimate of ET-capacity. Inhibition of
 731 respiration is observed at higher than optimum uncoupler concentrations. As a consequence of
 732 the nearly collapsed protonmotive force, the driving force is insufficient for phosphorylation,
 733 and $J_{P_{\infty}} = 0$.

734 **ROX state and *Rox*:** Besides the three fundamental coupling states of mitochondrial
 735 preparations, the state of residual oxygen consumption, ROX, is relevant to assess respiratory
 736 function. ROX is not a coupling state. The rate of residual oxygen consumption, *Rox*, is defined
 737 as O₂ consumption due to oxidative side reactions remaining after inhibition of ET—with
 738 rotenone, malonic acid and antimycin A. Cyanide and azide not only inhibit CIV but also
 739 several peroxidases involved in *Rox*. ROX represents a baseline that is used to correct
 740 mitochondrial respiration in defined coupling states. *Rox* is not necessarily equivalent to non-
 741 mitochondrial respiration, considering oxygen-consuming reactions in mitochondria not related
 742 to ET—such as oxygen consumption in reactions catalyzed by monoamine oxidases (type A
 743 and B), monooxygenases (cytochrome P450 monooxygenases), dioxygenase (sulfur
 744 dioxygenase and trimethyllysine dioxygenase), and several hydroxylases. Mitochondrial
 745 preparations, especially those obtained from liver, may be contaminated by peroxisomes. This
 746 fact makes the exact determination of mitochondrial oxygen consumption and mitochondria-
 747 associated generation of reactive oxygen species complicated (Schönfeld *et al.* 2009). The
 748 dependence of ROX-linked oxygen consumption needs to be studied in detail together with
 749 non-ET enzyme activities, availability of specific substrates, oxygen concentration, and
 750 electron leakage leading to the formation of reactive oxygen species.

751

752 2.3. Classical terminology for isolated mitochondria

753 ‘When a code is familiar enough, it ceases appearing like a code; one forgets that there
 754 is a decoding mechanism. The message is identical with its meaning’ (Hofstadter 1979).

755

756 Chance and Williams (1955; 1956) introduced five classical states of mitochondrial respiration
 757 and cytochrome redox states. **Table 3** shows a protocol with isolated mitochondria in a closed
 758 respirometric chamber, defining a sequence of respiratory states. States and rates are not
 759 specifically distinguished in this nomenclature.

760

Table 3. Metabolic states of mitochondria (Chance and Williams, 1956; Table V).

State	[O ₂]	ADP level	Substrate level	Respiration rate	Rate-limiting substance
1	>0	low	low	slow	ADP
2	>0	high	~0	slow	substrate
3	>0	high	high	fast	respiratory chain
4	>0	low	high	slow	ADP
5	0	high	high	0	oxygen

State 1 is obtained after addition of isolated mitochondria to air-saturated isoosmotic/isotonic respiration medium containing P_i, but no fuel substrates and no adenylates, *i.e.*, AMP, ADP, ATP.

State 2 is induced by addition of a ‘high’ concentration of ADP (typically 100 to 300 μM), which stimulates respiration transiently on the basis of endogenous fuel substrates and phosphorylates only a small portion of the added ADP. State 2 is then obtained at a low respiratory activity limited by exhausted endogenous fuel substrate availability (**Table 3**). If addition of specific inhibitors of respiratory complexes—such as rotenone—does not cause a further decline of oxygen consumption, State 2 is equivalent to the state of residual oxygen consumption, ROX (See below.). If inhibition is observed, undefined endogenous fuel substrates are a confounding factor of pathway control, contributing to the effect of subsequently externally added substrates and inhibitors. In contrast to the original protocol, an alternative sequence of titration steps is frequently applied, in which the alternative ‘State 2’ has an entirely different meaning, when this second state is induced by addition of fuel substrate without ADP (LEAK-state; in contrast to State 2 defined in **Table 1** as a ROX state), followed by addition of ADP.

State 3 is the state stimulated by addition of fuel substrates while the ADP concentration is still high (**Table 3**) and supports coupled energy transformation through oxidative phosphorylation. ‘High ADP’ is a concentration of ADP specifically selected to allow the measurement of State 3 to State 4 transitions of isolated mitochondria in a closed respirometric chamber. Repeated ADP titration re-establishes State 3 at ‘high ADP’. Starting at oxygen concentrations near air-saturation (ca. 200 μM O₂ at sea level and 37 °C), the total ADP concentration added must be low enough (typically 100 to 300 μM) to allow phosphorylation to ATP at a coupled rate of oxygen consumption that does not lead to oxygen depletion during the transition to State 4. In contrast, kinetically-saturating ADP concentrations usually are 10-fold higher than ‘high ADP’, *e.g.*, 2.5 mM in isolated mitochondria. The abbreviation State 3u is occasionally used in bioenergetics, to indicate the state of respiration after titration of an uncoupler, without sufficient emphasis on the fundamental difference between OXPHOS-capacity (*well-coupled* with an *endogenous* uncoupled component) and ET-capacity (*noncoupled*).

State 4 is a LEAK-state that is obtained only if the mitochondrial preparation is intact and well-coupled. Depletion of ADP by phosphorylation to ATP leads to a decline in the rate of oxygen consumption in the transition from State 3 to State 4. Under these conditions of State 4, a maximum protonmotive force and high ATP/ADP ratio are maintained. For calculation of P_»/O₂ ratios the gradual decline of Y_{P_»/O₂} towards diminishing [ADP] at State 4 must be taken into account (Gnaiger 2001). State 4 respiration, L_T (**Table 1**), reflects intrinsic proton leak and intrinsic ATP hydrolysis activity. Oxygen consumption in State 4 is an overestimation of LEAK-respiration if the contaminating ATP hydrolysis activity recycles some ATP to ADP, J_{P_«}, which stimulates respiration coupled to phosphorylation, J_{P_»} > 0. This can be tested by inhibition of the phosphorylation-pathway using oligomycin, ensuring that J_{P_»} = 0 (State 4o).

805 Alternatively, sequential ADP titrations re-establish State 3, followed by State 3 to State 4
 806 transitions while sufficient oxygen is available. Anoxia may be reached, however, before
 807 exhaustion of ADP (State 5).

808 **State 5** is the state after exhaustion of oxygen in a closed respirometric chamber.
 809 Diffusion of oxygen from the surroundings into the aqueous solution may be a confounding
 810 factor preventing complete anoxia (Gnaiger 2001). Chance and Williams (1955) provide an
 811 alternative definition of State 5, which gives it the different meaning of ROX versus anoxia:
 812 ‘State 5 may be obtained by antimycin A treatment or by anaerobiosis’.

813 In **Table 3**, only States 3 and 4 (and ‘State 2’ in the alternative protocol: addition of fuel
 814 substrates without ADP; not included in the table) are coupling control states, with the
 815 restriction that O₂ flux in State 3 may be limited kinetically by non-saturating ADP
 816 concentrations (**Table 1**).

817
 818

819 3. Normalization: fluxes and flows

820

821 3.1. Normalization: system or sample

822

823 The term *rate* is not sufficiently defined to be useful for reporting data (**Fig. 6**). The
 824 inconsistency of the meanings of rate becomes fully apparent when considering Galileo
 825 Galilei’s famous principle, that ‘bodies of different weight all fall at the same rate (have a
 826 constant acceleration)’ (Coopersmith 2010).

827

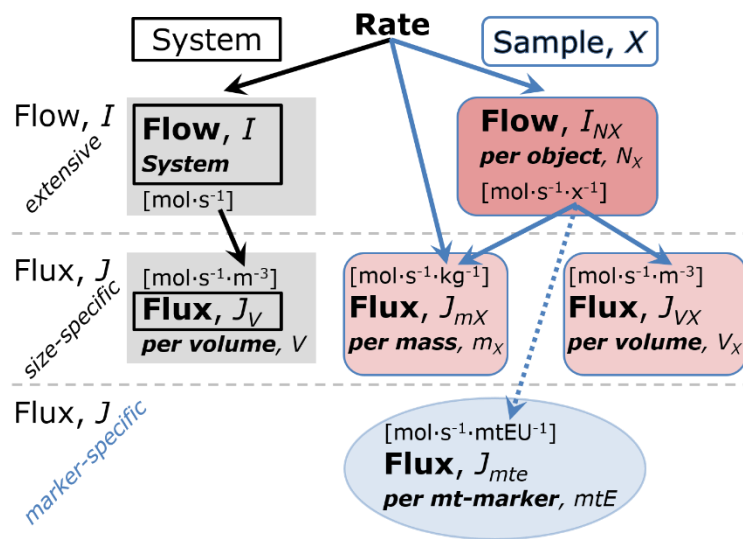
828 **Fig. 6. Different meanings of rate may lead to confusion, if the normalization is not sufficiently specified.** Results are frequently expressed as mass-specific flux, J_{mX} , per mg protein, dry or wet weight (mass). Cell volume, V_{cell} , may be used for normalization (volume-specific flux, $J_{V\text{cell}}$), which must be clearly distinguished from flow per cell, $I_{N\text{cell}}$, or flux, J_V , expressed for methodological reasons per volume of the measurement system. For details see **Table 4**.

843

844 **Flow per system, I :** In a generalization of electrical terms, flow as an extensive quantity (per system) is distinguished from flux as a size-specific quantity (per system size) (**Fig. 6**). Electric current is flow, I_{el} [$\text{A} \equiv \text{C}\cdot\text{s}^{-1}$] per system (extensive quantity). When dividing this extensive quantity by system size (cross-sectional area of a ‘wire’), a size-specific quantity is obtained, which is flux (current density), J_{el} [$\text{A}\cdot\text{m}^{-2} = \text{C}\cdot\text{s}^{-1}\cdot\text{m}^{-2}$].

849 **Extensive quantities:** An extensive quantity increases proportionally with system size. The magnitude of an extensive quantity is completely additive for non-interacting subsystems—such as mass or flow expressed per defined system. The magnitude of these quantities depends on the extent or size of the system (Cohen *et al.* 2008).

853 **Size-specific quantities:** ‘The adjective *specific* before the name of an extensive quantity is often used to mean *divided by mass*’ (Cohen *et al.* 2008). In this system-paradigm, mass-specific flux is flow divided by mass of the *system* (the total mass of everything within the measuring chamber). A mass-specific quantity is independent of the extent of non-interacting



856

857 homogenous subsystems. Tissue-specific quantities (related to the *sample* in contrast to the
 858 *system*) are of fundamental interest in comparative mitochondrial physiology, where *specific*
 859 refers to the *type of the sample* rather than *mass of the system*. The term *specific*, therefore, must
 860 be clarified; *sample-specific*, e.g., muscle mass-specific normalization, is distinguished from
 861 *system-specific* quantities (mass or volume; **Fig. 6**).
 862

863 **Box 2: Metabolic fluxes and flows: vectorial and scalar**

864
 865 We suggest to define: (1) *vectorial* fluxes, which are translocations as functions of
 866 *gradients* with direction in geometric space in continuous systems; (2) *vectorial* fluxes, which
 867 describe translocations in discontinuous systems and are restricted to information on
 868 *compartmental differences* (**Fig. 2**, transmembrane proton flux); and (3) *scalar* fluxes, which
 869 are transformations in a *homogenous* system (**Fig. 2**, catabolic O₂ flux, J_{kO_2}).

870 Vectorial transmembrane proton fluxes, $J_{\text{mH}^+\text{pos}}$ and $J_{\text{mH}^+\text{neg}}$, are analyzed in a
 871 heterogenous compartmental system as a quantity with *directional* but not *spatial* information.
 872 Translocation of protons across the mtIM has a defined direction, either from the negative
 873 compartment (matrix space; negative, neg-compartment) to the positive compartment (inter-
 874 membrane space; positive, pos-compartment) or *vice versa* (**Fig. 2**). The arrows defining the
 875 direction of the translocation between the two compartments may point upwards or downwards,
 876 right or left, without any implication that these are actual directions in space. The pos-
 877 compartment is neither above nor below the neg-compartment in a spatial sense, but can be
 878 visualized arbitrarily in a figure in the upper position (**Fig. 2**). In general, the *compartmental*
 879 *direction* of vectorial translocation from the neg-compartment to the pos-compartment is
 880 defined by assigning the initial and final state as *ergodynamic compartments*, $\text{H}^+_{\text{neg}} \rightarrow \text{H}^+_{\text{pos}}$ Or
 881 $0 = -1 \text{H}^+_{\text{neg}} + 1 \text{H}^+_{\text{pos}}$, related to work (erg = work) that must be performed to lift the proton from
 882 a lower to a higher electrochemical potential or from the lower to the higher ergodynamic
 883 compartment (Gnaiger 1993b).

884 In direct analogy to *vectorial* translocation, the direction of a *scalar* chemical reaction, A
 885 $\rightarrow \text{B}$ or $0 = -1 \text{A} + 1 \text{B}$, is defined by assigning substrates and products, A and B, as ergodynamic
 886 compartments. O₂ is defined as a substrate in respiratory O₂ consumption, which together with
 887 the fuel substrates comprises the substrate compartment of the catabolic reaction (**Fig. 2**).
 888 Volume-specific scalar O₂ flux is coupled to vectorial translocation, yielding the $\text{H}^+_{\text{pos}}/\text{O}_2$ ratio
 889 (**Fig. 1**).
 890

891 3.2. Normalization for system-size: flux per chamber volume

892
 893
 894 **System-specific flux, J :** The experimental system (experimental chamber) is part of the
 895 measurement apparatus, separated from the environment as an isolated, closed, open,
 896 isothermal or non-isothermal system (**Table 4**). On another level, we distinguish between (1)
 897 the *system* with volume V and mass m defined by the system boundaries, and (2) the *sample* or
 898 *objects* with volume V_X and mass m_X which are enclosed in the experimental chamber (**Fig. 6**).
 899 Metabolic O₂ flow per object, I_{X,O_2} , increases as the mass of the object is increased. Sample
 900 mass-specific O₂ flux, J_{mX,O_2} should be independent of the mass of the sample studied in the
 901 instrument chamber, but system volume-specific O₂ flux, J_{V,O_2} (per volume of the instrument
 902 chamber), should increase in direct proportion to the mass of the sample in the chamber.
 903 Whereas J_{V,O_2} depends on mass-concentration of the sample in the chamber, it should be
 904 independent of the chamber (system) volume at constant sample mass. There are practical
 905 limitations to increase the mass-concentration of the sample in the chamber, when one is
 906 concerned about crowding effects and instrumental time resolution.

907 When the reactor volume does not change during the reaction, which is typical for liquid
 908 phase reactions, the volume-specific *flux of a chemical reaction* r is the time derivative of the
 909 advancement of the reaction per unit volume, $J_{V,rB} = d_r\zeta_B/dt \cdot V^{-1}$ [(mol·s⁻¹)·L⁻¹]. The *rate of*
 910 *concentration change* is dc_B/dt [(mol·L⁻¹)·s⁻¹], where concentration is $c_B = n_B/V$. There is a
 911 difference between (1) J_{V,rO_2} [(mol·s⁻¹)·L⁻¹] and (2) rate of concentration change [(mol·L⁻¹)·s⁻¹].
 912 These merge to a single expression only in closed systems. In open systems, external fluxes
 913 (such as O₂ supply) are distinguished from internal transformations (catabolic flux, O₂
 914 consumption). In a closed system, external flows of all substances are zero and O₂ consumption
 915 (internal flow of catabolic reactions k), I_{kO_2} [pmol·s⁻¹], causes a decline of the amount of O₂ in
 916 the system, n_{O_2} [nmol]. Normalization of these quantities for the volume of the system, V [L \equiv
 917 dm³], yields volume-specific O₂ flux, $J_{V,kO_2} = I_{kO_2}/V$ [nmol·s⁻¹·L⁻¹], and O₂ concentration, [O₂]
 918 or $c_{O_2} = n_{O_2}/V$ [μ mol·L⁻¹ = μ M = nmol·mL⁻¹]. Instrumental background O₂ flux is due to external
 919 flux into a non-ideal closed respirometer; then total volume-specific flux has to be corrected for
 920 instrumental background O₂ flux—O₂ diffusion into or out of the instrumental chamber. J_{V,kO_2}
 921 is relevant mainly for methodological reasons and should be compared with the accuracy of
 922 instrumental resolution of background-corrected flux, e.g., ± 1 nmol·s⁻¹·L⁻¹ (Gnaiger 2001).
 923 ‘Metabolic’ or catabolic indicates O₂ flux, J_{kO_2} , corrected for: (1) instrumental background O₂
 924 flux; (2) chemical background O₂ flux due to autoxidation of chemical components added to
 925 the incubation medium; and (3) *Rox* for O₂-consuming side reactions unrelated to the catabolic
 926 pathway k .

927

928 3.3. Normalization: per sample

929

930 The challenges of measuring mitochondrial respiratory flux are matched by those of
 931 normalization. Application of common and defined units is required for direct transfer of
 932 reported results into a database. The second [s] is the *SI* unit for the base quantity *time*. It is also
 933 the standard time-unit used in solution chemical kinetics. A rate may be considered as the
 934 numerator and normalization as the complementary denominator, which are tightly linked in
 935 reporting the measurements in a format commensurate with the requirements of a database.
 936 Normalization (**Table 4**) is guided by physicochemical principles, methodological
 937 considerations, and conceptual strategies (**Fig. 7**).

938 **Sample concentration, C_{mX} :** Normalization for sample concentration is required to
 939 report respiratory data. Considering a tissue or cells as the sample, X , the sample mass is m_X
 940 [mg], which is frequently measured as wet or dry weight, W_w or W_d [mg], or as amount of tissue
 941 or cell protein, m_{Protein} . In the case of permeabilized tissues, cells, and homogenates, the sample
 942 concentration, $C_{mX} = m_X/V$ [g·L⁻¹ = mg·mL⁻¹], is the mass of the subsample of tissue that is
 943 transferred into the instrument chamber.

944 **Mass-specific flux, J_{mX,O_2} :** Mass-specific flux is obtained by expressing respiration per
 945 mass of sample, m_X [mg]. X is the type of sample—isolated mitochondria, tissue homogenate,
 946 permeabilized fibres or cells. Volume-specific flux is divided by mass concentration of X , J_{mX,O_2}
 947 = $J_{V,O_2}/C_{mX}$; or flow per cell is divided by mass per cell, $J_{m\text{cell},O_2} = I_{\text{cell},O_2}/M_{\text{cell}}$. If mass-specific
 948 O₂ flux is constant and independent of sample size (expressed as mass), then there is no
 949 interaction between the subsystems. A 1.5 mg and a 3.0 mg muscle sample respire at identical
 950 mass-specific flux. Mass-specific O₂ flux, however, may change with the mass of a tissue
 951 sample, cells or isolated mitochondria in the measuring chamber, in which the nature of the
 952 interaction becomes an issue. Therefore, cell density must be optimization, particularly in
 953 experiments carried out in wells, considering the confluency of the cell monolayer or clumps
 954 of cells (Salabei *et al.* 2014).

955 **Number concentration, C_{NX} :** C_{NX} is the experimental *number concentration* of sample
 956 X . In the case of cells or animals, e.g., nematodes, $C_{NX} = N_X/V$ [X·L⁻¹], where N_X is the number
 957 of cells or organisms in the chamber (**Table 4**).

Table 4. Sample concentrations and normalization of flux.

Expression	Symbol	Definition	Unit	Notes
Sample				
identity of sample	X	object: cell, tissue, animal, patient		
number of sample entities X	N_X	number of objects	x	
mass of sample X	m_X		kg	1
mass of object X	M_X	$M_X = m_X \cdot N_X^{-1}$	$\text{kg} \cdot \text{x}^{-1}$	1
Mitochondria				
mitochondria	mt	$X = \text{mt}$		
amount of mt-elements	mtE	quantity of mt-marker	mtEU	
Concentrations				
object number concentration	C_{NX}	$C_{NX} = N_X \cdot V^{-1}$	$\text{x} \cdot \text{m}^{-3}$	2
sample mass concentration	C_{mX}	$C_{mX} = m_X \cdot V^{-1}$	$\text{kg} \cdot \text{m}^{-3}$	
mitochondrial concentration	C_{mtE}	$C_{mtE} = mtE \cdot V^{-1}$	$\text{mtEU} \cdot \text{m}^{-3}$	3
specific mitochondrial density	D_{mtE}	$D_{mtE} = mtE \cdot m_X^{-1}$	$\text{mtEU} \cdot \text{kg}^{-1}$	4
mitochondrial content, mtE per object X	mtE_X	$mtE_X = mtE \cdot N_X^{-1}$	$\text{mtEU} \cdot \text{x}^{-1}$	5
O₂ flow and flux				
flow, system	I_{O_2}	internal flow	$\text{mol} \cdot \text{s}^{-1}$	6
volume-specific flux	J_{V,O_2}	$J_{V,O_2} = I_{O_2} \cdot V^{-1}$	$\text{mol} \cdot \text{s}^{-1} \cdot \text{m}^{-3}$	7
flow per object X	I_{X,O_2}	$I_{X,O_2} = J_{V,O_2} \cdot C_{NX}^{-1}$	$\text{mol} \cdot \text{s}^{-1} \cdot \text{x}^{-1}$	8
mass-specific flux	J_{mX,O_2}	$J_{mX,O_2} = J_{V,O_2} \cdot C_{mX}^{-1}$	$\text{mol} \cdot \text{s}^{-1} \cdot \text{kg}^{-1}$	9
mitochondria-specific flux	J_{mtE,O_2}	$J_{mtE,O_2} = J_{V,O_2} \cdot C_{mtE}^{-1}$	$\text{mol} \cdot \text{s}^{-1} \cdot \text{mtEU}^{-1}$	10

- 960 1 The SI prefix k is used for the SI base unit of mass (kg = 1,000 g). In praxis, various SI prefixes are
961 used for convenience, to make numbers easily readable, e.g., 1 mg tissue, cell or mitochondrial mass
962 instead of 0.000001 kg.
- 963 2 In case sample $X = \text{cells}$, the object number concentration is $C_{N_{\text{cell}}} = N_{\text{cell}} \cdot V^{-1}$, and volume may be
964 expressed in [$\text{dm}^3 \equiv \text{L}$] or [$\text{cm}^3 = \text{mL}$]. See **Table 5** for different object types.
- 965 3 mt-concentration is an experimental variable, dependent on sample concentration: (1) $C_{mtE} = mtE \cdot V^{-1}$;
966 (2) $C_{mtE} = mtE_X \cdot C_{NX}$; (3) $C_{mtE} = C_{mX} \cdot D_{mtE}$.
- 967 4 If the amount of mitochondria, mtE , is expressed as mitochondrial mass, then D_{mtE} is the mass
968 fraction of mitochondria in the sample. If mtE is expressed as mitochondrial volume, V_{mt} , and the
969 mass of sample, m_X , is replaced by volume of sample, V_X , then D_{mtE} is the volume fraction of
970 mitochondria in the sample.
- 971 5 $mtE_X = mtE \cdot N_X^{-1} = C_{mtE} \cdot C_{NX}^{-1}$.
- 972 6 O₂ can be replaced by other chemicals B to study different reactions, e.g., ATP, H₂O₂, or
973 compartmental translocations, e.g., Ca²⁺.
- 974 7 I_{O_2} and V are defined per instrument chamber as a system of constant volume (and constant
975 temperature), which may be closed or open. I_{O_2} is abbreviated for I_{O_2r} —the metabolic or internal O₂
976 flow of the chemical reaction r in which O₂ is consumed—hence the negative stoichiometric number,
977 $\nu_{O_2} = -1$. $I_{O_2r} = d_r n_{O_2} / dt \cdot \nu_{O_2}^{-1}$. If r includes all chemical reactions in which O₂ participates, then $d_r n_{O_2} = dn_{O_2}$
978 $- d_e n_{O_2}$, where dn_{O_2} is the change in the amount of O₂ in the instrument chamber and $d_e n_{O_2}$ is the
979 amount of O₂ added externally to the system. At steady state, by definition $dn_{O_2} = 0$, hence $d_r n_{O_2} = -$
980 $d_e n_{O_2}$.
- 981 8 J_{V,O_2} is an experimental variable, expressed per volume of the instrument chamber.
- 982 9 I_{X,O_2} is a physiological variable, depending on the size of entity X .
- 983 10 There are many ways to normalize for a mitochondrial marker, that are used in different experimental
984 approaches: (1) $J_{mtE,O_2} = J_{V,O_2} \cdot C_{mtE}^{-1}$; (2) $J_{mtE,O_2} = J_{V,O_2} \cdot C_{mX}^{-1} \cdot D_{mtE}^{-1} = J_{mX,O_2} \cdot D_{mtE}^{-1}$; (3) $J_{mtE,O_2} =$
985 $J_{V,O_2} \cdot C_{NX}^{-1} \cdot mtE_X^{-1} = I_{X,O_2} \cdot mtE_X^{-1}$; (4) $J_{mtE,O_2} = I_{O_2} \cdot mtE^{-1}$. The mt-elemental unit [mtEU] varies between
986 different mt-markers.

987

Table 5. Sample types, X, abbreviations, and quantification.

Identity of sample	X	N_X	Mass ^a	Volume	mt-Marker
mitochondrial preparation	Mtprep	[x]	[kg]	[m ³]	[mtEU]
isolated mitochondria	imt		m_{mt}	V_{mt}	mtE
tissue homogenate	thom		m_{thom}		mtE_{thom}
permeabilized tissue	pti		m_{pti}		mtE_{pti}
permeabilized fibre	pfi		m_{pfi}		mtE_{pfi}
permeabilized cell	pce	N_{pce}	M_{pce}	V_{pce}	mtE_{pce}
intact cell	ce	N_{ce}	M_{ce}	V_{ce}	mtE_{ce}
organism	org	N_{org}	M_{org}	V_{org}	

988

^a Instead of mass, frequently the wet weight or dry weight is stated, W_w or W_d .

989

m_X is mass of the sample [kg], M_X is mass of the object [kg·x⁻¹].

990

991

Flow per object, I_{X,O_2} : A special case of normalization is encountered in respiratory studies with permeabilized (or intact) cells. If respiration is expressed per cell, the O₂ flow per measurement system is replaced by the O₂ flow per cell, I_{cell,O_2} (**Table 4**). O₂ flow can be calculated from volume-specific O₂ flux, J_{V,O_2} [nmol·s⁻¹·L⁻¹] (per V of the measurement chamber [L]), divided by the number concentration of cells, $C_{N_{ce}} = N_{ce}/V$ [cell·L⁻¹], where N_{ce} is the number of cells in the chamber. Cellular O₂ flow can be compared between cells of identical size. To take into account changes and differences in cell size, normalization is required to obtain cell size-specific or mitochondrial marker-specific O₂ flux (Renner *et al.* 2003).

992

993

994

995

996

997

998

999

The complexity changes when the sample is a whole organism studied as an experimental model. The scaling law in respiratory physiology reveals a strong interaction of O₂ consumption and individual body mass of an organism, since *basal* metabolic rate (flow) does not increase linearly with body mass, whereas *maximum* mass-specific O₂ flux, \dot{V}_{O_2max} or \dot{V}_{O_2peak} , is approximately constant across a large range of individual body mass (Weibel and Hoppeler 2005), with individuals, breeds, and species deviating substantially from this relationship. \dot{V}_{O_2peak} of human endurance athletes is 60 to 80 mL O₂·min⁻¹·kg⁻¹ body mass, converted to J_{M,O_2peak} of 45 to 60 nmol·s⁻¹·g⁻¹ (Gnaiger 2014; **Table 6**).

1000

1001

1002

1003

1004

1005

1006

1007

1008

3.4. Normalization for mitochondrial content

1009

1010

1011

1012

1013

1014

1015

1016

1017

1018

Tissues can contain multiple cell populations that may have distinct mitochondrial subtypes. Mitochondria undergo dynamic fission and fusion cycles, and can exist in multiple stages and sizes which may be altered by a range of factors. The isolation of mitochondria (often achieved through differential centrifugation) can therefore yield a subsample of the mitochondrial types present in a tissue, depending on isolation protocols utilized (*e.g.*, centrifugation speed). This possible bias should be taken into account when planning experiments using isolated mitochondria. Different sizes of mitochondria are enriched at specific centrifugation speeds, which is used for isolation of mitochondrial subpopulations.

1019

1020

1021

1022

1023

1024

1025

Part of the mitochondrial content of a tissue is lost during preparation of isolated mitochondria. The fraction of mitochondria in the isolate is expressed as mitochondrial recovery. At a high mitochondrial recovery the sample of isolated mitochondria is more representative of the total mitochondrial population than in preparations characterized by low recovery. Determination of the mitochondrial recovery and yield is based on measurement of the concentration of a mitochondrial marker in the tissue homogenate, $C_{mtE,thom}$, which simultaneously provides information on the specific mitochondrial density in the sample.

1026

1027

1028

Normalization is a problematic subject; it is essential to consider the question of the study. If the study aims at comparing tissue performance—such as the effects of a treatment on a specific tissue, then normalization can be successful, using tissue mass or protein content, for example. However, if the aim is to find differences on mitochondrial function independent of

1029 mitochondrial density (**Table 4**), then normalization to a mitochondrial marker is imperative
 1030 (**Fig. 7**). One cannot assume that quantitative changes in various markers—such as
 1031 mitochondrial proteins—necessarily occur in parallel with one another. It should be established
 1032 that the marker chosen is not selectively altered by the performed treatment. In conclusion, the
 1033 normalization must reflect the question under investigation to reach a satisfying answer. On the
 1034 other hand, the goal of comparing results across projects and institutions requires
 1035 standardization on normalization for entry into a databank.
 1036

Flow, Performance	=	Element function	x	Element density	x	Size of entity
$\frac{\text{mol}\cdot\text{s}^{-1}}{x}$	=	$\frac{\text{mol}\cdot\text{s}^{-1}}{x_{\text{mte}}}$	·	$\frac{x_{\text{mte}}}{\text{kg}}$	·	$\frac{\text{kg}}{x}$

A	Flow	=	mt-specific flux	x	mt-structure, functional elements
	I_{X,O_2}	=	J_{mte,O_2}	·	mte_X
					$\frac{\text{mte}_X}{M_X} \cdot M_X$

	I_{X,O_2}	=	J_{mte,O_2}	·	D_{mte}	·	M_X
	$\frac{I_{X,O_2}}{M_X}$	=	$\frac{I_{X,O_2}}{\text{mte}_X}$	·	$\frac{\text{mte}_X}{M_X}$		

B	Flow	=	Entity mass- specific flux	x	Mass of entity
	I_{X,O_2}	=	J_{mX,O_2}	·	M_X

1037
 1038 **Fig. 7. Structure-function analysis of performance of an organism, organ or tissue, or a**
 1039 **cell (sample entity, X). O₂ flow, I_{X,O_2} , is the product of performance per functional element**
 1040 **(element function, mitochondria-specific flux), element density (mitochondrial density,**
 1041 **D_{mtE}), and size of entity X (mass, M_X). (A) Structured analysis: performance is the product of**
 1042 **mitochondrial function (mt-specific flux) and structure (functional elements; D_{mtE} times mass**
 1043 **of X). (B) Unstructured analysis: performance is the product of entity mass-specific flux, J_{mX,O_2}**
 1044 **$= I_{X,O_2}/M_X = I_{O_2}/m_X$ [$\text{mol}\cdot\text{s}^{-1}\cdot\text{kg}^{-1}$] and size of entity, expressed as mass of X; $M_X = m_X\cdot N_X^{-1}$**
 1045 **[$\text{kg}\cdot\text{x}^{-1}$]. See **Table 4** for further explanation of quantities and units. Modified from Gnaiger**
 1046 **(2014).**
 1047

1048 **Mitochondrial concentration, C_{mtE} , and mitochondrial markers:** Mitochondrial
 1049 organelles comprise a dynamic cellular reticulum in various states of fusion and fission. Hence,
 1050 the definition of an "amount" of mitochondria is often misconceived: mitochondria cannot be
 1051 counted reliably as a number of occurring elements. Therefore, quantification of the "amount"
 1052 of mitochondria depends on the measurement of chosen mitochondrial markers. 'Mitochondria
 1053 are the structural and functional elemental units of cell respiration' (Gnaiger 2014). The
 1054 quantity of a mitochondrial marker can reflect the amount of *mitochondrial elements*, *mtE*,
 1055 expressed in various mitochondrial elemental units [mtEU] specific for each measured mt-
 1056 marker (**Table 4**). However, since mitochondrial quality may change in response to stimuli—
 1057 particularly in mitochondrial dysfunction and after exercise training (Pesta *et al.* 2011; Campos
 1058 *et al.* 2017)—some markers can vary while others are unchanged: (1) Mitochondrial volume
 1059 and membrane area are structural markers, whereas mitochondrial protein mass is frequently
 1060 used as a marker for isolated mitochondria. (2) Molecular and enzymatic mitochondrial markers
 1061 (amounts or activities) can be selected as matrix markers, *e.g.*, citrate synthase activity, mtDNA;

1062 mtIM-markers, *e.g.*, cytochrome *c* oxidase activity, *aa*₃ content, cardiolipin, or mtOM-markers,
 1063 *e.g.*, TOM20. (3) Extending the measurement of mitochondrial marker enzyme activity to
 1064 mitochondrial pathway capacity, ET- or OXPHOS-capacity can be considered as an integrative
 1065 functional mitochondrial marker.

1066 Depending on the type of mitochondrial marker, the mitochondrial elements, *mtE*, are
 1067 expressed in marker-specific units. Mitochondrial concentration in the measurement chamber
 1068 and the tissue of origin are quantified as (1) a quantity for normalization in functional analyses,
 1069 C_{mtE} , and (2) a physiological output that is the result of mitochondrial biogenesis and
 1070 degradation, D_{mtE} , respectively (Table 4). It is recommended, therefore, to distinguish
 1071 *experimental mitochondrial concentration*, $C_{mtE} = mtE/V$ and *physiological mitochondrial*
 1072 *density*, $D_{mtE} = mtE/m_X$. Then mitochondrial density is the amount of mitochondrial elements
 1073 per mass of tissue, which is a biological variable (Fig. 7). The experimental variable is
 1074 mitochondrial density multiplied by sample mass concentration in the measuring chamber, C_{mtE}
 1075 $= D_{mtE} \cdot C_{mX}$, or mitochondrial content multiplied by sample number concentration, $C_{mtE} =$
 1076 $mtE_X \cdot C_{NX}$ (Table 4).

1077 **Mitochondria-specific flux, J_{mtE,O_2} :** Volume-specific metabolic O₂ flux depends on: (1)
 1078 the sample concentration in the volume of the instrument chamber, C_{mX} , or C_{NX} ; (2) the
 1079 mitochondrial density in the sample, $D_{mtE} = mtE/m_X$ or $mtE_X = mtE/N_X$; and (3) the specific
 1080 mitochondrial activity or performance per elemental mitochondrial unit, $J_{mtE,O_2} = J_{V,O_2}/C_{mtE}$
 1081 [mol·s⁻¹·mtEU⁻¹] (Table 4). Obviously, the numerical results for J_{mtE,O_2} vary with the type of
 1082 mitochondrial marker chosen for measurement of *mtE* and $C_{mtE} = mtE/V$ [mtEU·m⁻³].

1083

1084 3.5. Evaluation of mitochondrial markers

1085

1086 Different methods are implicated in the quantification of mitochondrial markers and have
 1087 different strengths. Some problems are common for all mitochondrial markers, *mtE*: (1)
 1088 Accuracy of measurement is crucial, since even a highly accurate and reproducible
 1089 measurement of O₂ flux results in an inaccurate and noisy expression normalized for a biased
 1090 and noisy measurement of a mitochondrial marker. This problem is acute in mitochondrial
 1091 respiration because the denominators used (the mitochondrial markers) are often small moieties
 1092 of which accurate and precise determination is difficult. This problem can be avoided when O₂
 1093 fluxes measured in substrate-uncoupler-inhibitor titration protocols are normalized for flux in
 1094 a defined respiratory reference state, which is used as an *internal* marker and yields flux control
 1095 ratios, *FCRs*. *FCRs* are independent of any *externally* measured markers and, therefore, are
 1096 statistically robust, considering the limitations of ratios in general (Jasienski and Bazzaz 1999).
 1097 *FCRs* indicate qualitative changes of mitochondrial respiratory control, with highest
 1098 quantitative resolution, separating the effect of mitochondrial density or concentration on J_{mX,O_2}
 1099 and I_{X,O_2} from that of function per elemental mitochondrial marker, J_{mtE,O_2} (Pesta *et al.* 2011;
 1100 Gnaiger 2014). (2) If mitochondrial quality does not change and only the amount of
 1101 mitochondria varies as a determinant of mass-specific flux, any marker is equally qualified in
 1102 principle; then in practice selection of the optimum marker depends only on the accuracy and
 1103 precision of measurement of the mitochondrial marker. (3) If mitochondrial flux control ratios
 1104 change, then there may not be any best mitochondrial marker. In general, measurement of
 1105 multiple mitochondrial markers enables a comparison and evaluation of normalization for a
 1106 variety of mitochondrial markers. Particularly during postnatal development, the activity of
 1107 marker enzymes—such as cytochrome *c* oxidase and citrate synthase—follows different time
 1108 courses (Drahota *et al.* 2004). Evaluation of mitochondrial markers in healthy controls is
 1109 insufficient for providing guidelines for application in the diagnosis of pathological states and
 1110 specific treatments.

1111 In line with the concept of the respiratory control ratio (Chance and Williams 1955a), the
 1112 most readily used normalization is that of flux control ratios and flux control factors (Gnaiger

1113 2014). Selection of the state of maximum flux in a protocol as the reference state has the
 1114 advantages of: (1) internal normalization; (2) statistical linearization of the response in the range
 1115 of 0 to 1; and (3) consideration of maximum flux for integrating a large number of elemental
 1116 steps in the OXPHOS- or ET-pathways. This reduces the risk of selecting a functional marker
 1117 that is specifically altered by the treatment or pathology, yet increases the chance that the highly
 1118 integrative pathway is disproportionately affected, *e.g.*, the OXPHOS- rather than ET-pathway
 1119 in case of an enzymatic defect in the phosphorylation-pathway. In this case, additional
 1120 information can be obtained by reporting flux control ratios based on a reference state which
 1121 indicates stable tissue-mass specific flux. Stereological determination of mitochondrial content
 1122 via two-dimensional transmission electron microscopy can have limitations due to the dynamics
 1123 of mitochondrial size (Meinild Lundby *et al.* 2017). Accurate determination of three-
 1124 dimensional volume by two-dimensional microscopy can be both time consuming and
 1125 statistically challenging (Larsen *et al.* 2012).

1126 The validity of using mitochondrial marker enzymes (citrate synthase activity, Complex
 1127 I–IV amount or activity) for normalization of flux is limited in part by the same factors that
 1128 apply to flux control ratios. Strong correlations between various mitochondrial markers and
 1129 citrate synthase activity (Reichmann *et al.* 1985; Boushel *et al.* 2007; Mogensen *et al.* 2007)
 1130 are expected in a specific tissue of healthy subjects and in disease states not specifically
 1131 targeting citrate synthase. Citrate synthase activity is acutely modifiable by exercise
 1132 (Tonkonogi *et al.* 1997; Leek *et al.* 2001). Evaluation of mitochondrial markers related to a
 1133 selected age and sex cohort cannot be extrapolated to provide recommendations for
 1134 normalization in respirometric diagnosis of disease, in different states of development and
 1135 ageing, different cell types, tissues, and species. mtDNA normalized to nDNA via qPCR is
 1136 correlated to functional mitochondrial markers including OXPHOS- and ET-capacity in some
 1137 cases (Puntschart *et al.* 1995; Wang *et al.* 1999; Menshikova *et al.* 2006; Boushel *et al.* 2007),
 1138 but lack of such correlations have been reported (Menshikova *et al.* 2005; Schultz and Wiesner
 1139 2000; Pesta *et al.* 2011). Several studies indicate a strong correlation between cardiolipin
 1140 content and increase in mitochondrial function with exercise (Menshikova *et al.* 2005;
 1141 Menshikova *et al.* 2007; Larsen *et al.* 2012; Faber *et al.* 2014), but its use as a general
 1142 mitochondrial biomarker in disease remains questionable.

1143 3.6. Conversion: units

1144 Many different units have been used to report the rate of oxygen consumption, OCR
 1145 (Table 6). *SI* base units provide the common reference to introduce the theoretical principles
 1146 (Fig. 6), and are used with appropriately chosen *SI* prefixes to express numerical data in the
 1147 most practical format, with an effort towards unification within specific areas of application
 1148 (Table 7). Reporting data in *SI* units—including the mole [mol], coulomb [C], joule [J], and
 1149 second [s]—should be encouraged, particularly by journals which propose the use of *SI* units.

1150 Although volume is expressed as m^3 using the *SI* base unit, the litre [dm^3] is a
 1151 conventional unit of volume for concentration and is used for most solution chemical kinetics.
 1152 If one multiplies $I_{\text{cell},\text{O}_2}$ by $C_{N_{\text{cell}}}$, then the result will not only be the amount of O_2 [mol]
 1153 consumed per time [s^{-1}] in one litre [L^{-1}], but also the change in the concentration of oxygen per
 1154 second (for any volume of an ideally closed system). This is ideal for kinetic modeling as it
 1155 blends with chemical rate equations where concentrations are typically expressed in $\text{mol}\cdot\text{L}^{-1}$
 1156 (Wagner *et al.* 2011). In studies of multinuclear cells—such as differentiated skeletal muscle
 1157 cells—it is easy to determine the number of nuclei but not the total number of cells. A
 1158 generalized concept, therefore, is obtained by substituting cells by nuclei as the sample entity.
 1159 This does not hold, however, for enucleated platelets.

1160
1161
1162

1163
1164
1165
1166**Table 6. Conversion of various units used in respirometry and ergometry.** e^- is the number of electrons or reducing equivalents. z_B is the charge number of entity B.

1 Unit	x	Multiplication factor	SI-unit	Note
ng.atom O \cdot s $^{-1}$	(2 e^-)	0.5	nmol O $_2$ \cdot s $^{-1}$	
ng.atom O \cdot min $^{-1}$	(2 e^-)	8.33	pmol O $_2$ \cdot s $^{-1}$	
natom O \cdot min $^{-1}$	(2 e^-)	8.33	pmol O $_2$ \cdot s $^{-1}$	
nmol O $_2$ \cdot min $^{-1}$	(4 e^-)	16.67	pmol O $_2$ \cdot s $^{-1}$	
nmol O $_2$ \cdot h $^{-1}$	(4 e^-)	0.2778	pmol O $_2$ \cdot s $^{-1}$	
mL O $_2$ \cdot min $^{-1}$ at STPD ^a		0.744	μ mol O $_2$ \cdot s $^{-1}$	1
W = J/s at -470 kJ/mol O $_2$		-2.128	μ mol O $_2$ \cdot s $^{-1}$	
mA = mC \cdot s $^{-1}$	($z_{H^+} = 1$)	10.36	nmol H $^+$ \cdot s $^{-1}$	2
mA = mC \cdot s $^{-1}$	($z_{O_2} = 4$)	2.59	nmol O $_2$ \cdot s $^{-1}$	2
nmol H $^+$ \cdot s $^{-1}$	($z_{H^+} = 1$)	0.09649	mA	3
nmol O $_2$ \cdot s $^{-1}$	($z_{O_2} = 4$)	0.38594	mA	3

1167
1168
1169
1170
1171
1172
1173
1174
1175
1176

- 1 At standard temperature and pressure dry (STPD: 0 °C = 273.15 K and 1 atm = 101.325 kPa = 760 mmHg), the molar volume of an ideal gas, V_m , and V_{m,O_2} is 22.414 and 22.392 L \cdot mol $^{-1}$, respectively. Rounded to three decimal places, both values yield the conversion factor of 0.744. For comparison at NTPD (20 °C), V_{m,O_2} is 24.038 L \cdot mol $^{-1}$. Note that the SI standard pressure is 100 kPa.
- 2 The multiplication factor is $10^6/(z_B \cdot F)$.
- 3 The multiplication factor is $z_B \cdot F/10^6$.

Table 7. Conversion of units with preservation of numerical values.

Name	Frequently used unit	Equivalent unit	Note
volume-specific flux, J_{V,O_2}	pmol \cdot s $^{-1}$ \cdot mL $^{-1}$	nmol \cdot s $^{-1}$ \cdot L $^{-1}$	1
	mmol \cdot s $^{-1}$ \cdot L $^{-1}$	mol \cdot s $^{-1}$ \cdot m $^{-3}$	
cell-specific flow, I_{O_2}	pmol \cdot s $^{-1}$ \cdot 10 $^{-6}$ cells	amol \cdot s $^{-1}$ \cdot cell $^{-1}$	2
	pmol \cdot s $^{-1}$ \cdot 10 $^{-9}$ cells	zmol \cdot s $^{-1}$ \cdot cell $^{-1}$	3
cell number concentration, C_{Nce}	10 6 cells \cdot mL $^{-1}$	10 9 cells \cdot L $^{-1}$	
mitochondrial protein concentration, C_{mtE}	0.1 mg \cdot mL $^{-1}$	0.1 g \cdot L $^{-1}$	
mass-specific flux, J_{m,O_2}	pmol \cdot s $^{-1}$ \cdot mg $^{-1}$	nmol \cdot s $^{-1}$ \cdot g $^{-1}$	4
catabolic power, P_k	μ W \cdot 10 $^{-6}$ cells	pW \cdot cell $^{-1}$	1
Volume	1,000 L	m 3 (1,000 kg)	
	L	dm 3 (kg)	
	mL	cm 3 (g)	
	μ L	mm 3 (mg)	
	fL	μ m 3 (pg)	5
amount of substance concentration	M = mol \cdot L $^{-1}$	mol \cdot dm $^{-3}$	

1177
1178
1179
1180
1181

- 1 pmol: picomole = 10 $^{-12}$ mol
- 2 amol: attomole = 10 $^{-18}$ mol
- 3 zmol: zeptomole = 10 $^{-21}$ mol
- 4 nmol: nanomole = 10 $^{-9}$ mol
- 5 fL: femtolitre = 10 $^{-15}$ L

1182 For studies of cells, we recommend that respiration be expressed, as far as possible, as:
 1183 (1) O_2 flux normalized for a mitochondrial marker, for separation of the effects of mitochondrial
 1184 quality and content on cell respiration (this includes *FCRs* as a normalization for a functional
 1185 mitochondrial marker); (2) O_2 flux in units of cell volume or mass, for comparison of respiration
 1186 of cells with different cell size (Renner *et al.* 2003) and with studies on tissue preparations, and
 1187 (3) O_2 flow in units of attomole (10^{-18} mol) of O_2 consumed in a second by each cell
 1188 [$\text{amol}\cdot\text{s}^{-1}\cdot\text{cell}^{-1}$], numerically equivalent to [$\text{pmol}\cdot\text{s}^{-1}\cdot 10^{-6}$ cells]. This convention allows
 1189 information to be easily used when designing experiments in which oxygen consumption must
 1190 be considered. For example, to estimate the volume-specific O_2 flux in an instrument chamber
 1191 that would be expected at a particular cell number concentration, one simply needs to multiply
 1192 the flow per cell by the number of cells per volume of interest. This provides the amount of O_2
 1193 [mol] consumed per time [s^{-1}] per unit volume [L^{-1}]. At an O_2 flow of $100 \text{ amol}\cdot\text{s}^{-1}\cdot\text{cell}^{-1}$ and a
 1194 cell density of $10^9 \text{ cells}\cdot\text{L}^{-1}$ ($10^6 \text{ cells}\cdot\text{mL}^{-1}$), the volume-specific O_2 flux is $100 \text{ nmol}\cdot\text{s}^{-1}\cdot\text{L}^{-1}$ (100
 1195 $\text{pmol}\cdot\text{s}^{-1}\cdot\text{mL}^{-1}$).

1196 ET-capacity in human cell types including HEK 293, primary HUVEC and fibroblasts
 1197 ranges from 50 to $180 \text{ amol}\cdot\text{s}^{-1}\cdot\text{cell}^{-1}$, measured in intact cells in the noncoupled state (see
 1198 Gnaiger 2014). At $100 \text{ amol}\cdot\text{s}^{-1}\cdot\text{cell}^{-1}$ corrected for *Rox*, the current across the mt-membranes,
 1199 I_{eH^+} , approximates $193 \text{ pA}\cdot\text{cell}^{-1}$ or 0.2 nA per cell. See Rich (2003) for an extension of
 1200 quantitative bioenergetics from the molecular to the human scale, with a transmembrane proton
 1201 flux equivalent to 520 A in an adult at a catabolic power of -110 W. Modelling approaches
 1202 illustrate the link between protonmotive force and currents (Willis *et al.* 2016).

1203 We consider isolated mitochondria as powerhouses and proton pumps as molecular
 1204 machines to relate experimental results to energy metabolism of the intact cell. The cellular
 1205 P_{\gg}/O_2 based on oxidation of glycogen is increased by the glycolytic (fermentative) substrate-
 1206 level phosphorylation of 3 P_{\gg}/Glyc or 0.5 mol P_{\gg} for each mol O_2 consumed in the complete
 1207 oxidation of a mol glycosyl unit (Glyc). Adding 0.5 to the mitochondrial P_{\gg}/O_2 ratio of 5.4
 1208 yields a bioenergetic cell physiological P_{\gg}/O_2 ratio close to 6. Two NADH equivalents are
 1209 formed during glycolysis and transported from the cytosol into the mitochondrial matrix, either
 1210 by the malate-aspartate shuttle or by the glycerophosphate shuttle resulting in different
 1211 theoretical yields of ATP generated by mitochondria, the energetic cost of which potentially
 1212 must be taken into account. Considering also substrate-level phosphorylation in the TCA cycle,
 1213 this high P_{\gg}/O_2 ratio not only reflects proton translocation and OXPHOS studied in isolation,
 1214 but integrates mitochondrial physiology with energy transformation in the living cell (Gnaiger
 1215 1993a).

1216
1217

1218 4. Conclusions

1219

1220 MitoEAGLE can serve as a gateway to better diagnose mitochondrial respiratory defects
 1221 linked to genetic variation, age-related health risks, sex-specific mitochondrial performance,
 1222 lifestyle with its effects on degenerative diseases, and thermal and chemical environment. The
 1223 present recommendations on coupling control states and rates, linked to the concept of the
 1224 protonmotive force, are focused on studies with mitochondrial preparations. These will be
 1225 extended in a series of reports on pathway control of mitochondrial respiration, respiratory
 1226 states in intact cells, and harmonization of experimental procedures.

1227 The optimal choice for expressing mitochondrial and cell respiration (**Box 3**) as O_2 flow
 1228 per biological system, and normalization for specific tissue-markers (volume, mass, protein)
 1229 and mitochondrial markers (volume, protein, content, mtDNA, activity of marker enzymes,
 1230 respiratory reference state) is guided by the scientific question under study. Interpretation of
 1231 the obtained data depends critically on appropriate normalization, and therefore reporting rates
 1232 merely as $\text{nmol}\cdot\text{s}^{-1}$ is discouraged, since it restricts the analysis to intra-experimental

Table 8. Terms, symbols, and units.

Term	Symbol	Unit	Links and comments
alternative quinol oxidase	AOX		Fig. 1
amount of substance B	n_B	[mol]	
Complexes I to IV	CI to CIV		respiratory ET Complexes; Fig. 1
concentration of substance B	$c_B = n_B \cdot V^{-1}$; [B]	[mol·m ⁻³]	Box 2
electron transfer system	ETS		Fig. 1, Fig. 4
flow, for substance B	I_B	[mol·s ⁻¹]	system-related extensive quantity; Fig. 6
flux, for substance B	J_B	<i>varies</i>	size-specific quantity; Fig. 6
inorganic phosphate	P_i		Fig. 2
LEAK	LEAK		Tab. 1, Fig. 4
mass of sample X	m_X	[kg]	Tab. 4
mass of entity X	M_X	[kg]	mass of object X; Tab. 4
MITOCARTA			https://www.broadinstitute.org/scientific-community/science/programs/metabolic-disease-program/publications/mitocarta/mitocarta-in-0
MitoPedia			http://www.bioblast.at/index.php/MitoPedia
mitochondria or mitochondrial	mt		Box 1
mitochondrial DNA	mtDNA		Box 1
mitochondrial concentration	$C_{mtE} = mtE \cdot V^{-1}$	[mtEU·m ⁻³]	Tab. 4
mitochondrial content	$mtE_X = mtE \cdot N_X^{-1}$	[mtEU·x ⁻¹]	Tab. 4
mitochondrial elemental unit	mtEU	<i>varies</i>	Tab. 4, specific units for mt-marker
mitochondrial inner membrane	mtIM		MIM is widely used; the first M is replaced by mt; Box 1
mitochondrial outer membrane	mtOM		MOM is widely used; the first M is replaced by mt; Box 1
mitochondrial recovery	Y_{mtE}		fraction of <i>mtE</i> recovered in sample from the tissue of origin
mitochondrial yield	$Y_{mtE/m}$		$Y_{mtE/m} = Y_{mtE} \cdot D_{mtE}$
negative	neg		Fig. 2
number concentration of X	C_{NX}	[x·m ⁻³]	Tab. 4
number of entities X	N_X	[x]	Tab. 4, Fig. 7
number of entity B	N_B	[x]	Tab. 4
oxidative phosphorylation	OXPHOS		Tab. 1, Fig. 4
oxygen concentration	$c_{O_2} = n_{O_2} \cdot V^{-1}$; [O ₂]	[mol·m ⁻³]	Section 3.2
phosphorylation of ADP to ATP	P»		Section 2.2
positive	pos		Fig. 2
proton in the negative compartment	H ⁺ _{neg}		Fig. 2
proton in the positive compartment	H ⁺ _{pos}		Fig. 2
rate of electron transfer in ET state	E		ET-capacity; Tab. 1
rate of LEAK respiration	L		Tab. 1
rate of oxidative phosphorylation	P		OXPHOS capacity; Tab. 1
rate of residual oxygen consumption	ROx		Tab. 1
residual oxygen consumption	ROX		Tab. 1
specific mitochondrial density	$D_{mtE} = mtE \cdot m_X^{-1}$	[mtEU·kg ⁻¹]	Tab. 7
volume	V	[m ³]	
weight, dry weight	W_d	[kg]	used as mass of sample X; Fig. 6
weight, wet weight	W_w	[kg]	used as mass of sample X; Fig. 6

1288
1289 comparison of relative (qualitative) differences. Expressing O₂ consumption per cell may not
1290 be possible when dealing with tissues. For studies with mitochondrial preparations, we
1291 recommend that normalizations be provided as far as possible: (1) on a per cell basis as O₂ flow
1292 (a biophysical normalization); (2) per g cell or tissue protein, or per cell or tissue mass as mass-
1293 specific O₂ flux (a cellular normalization); and (3) per mitochondrial marker as mt-specific flux

1294 (a mitochondrial normalization). With information on cell size and the use of multiple
 1295 normalizations, maximum potential information is available (Renner *et al.* 2003; Wagner *et al.*
 1296 2011; Gnaiger 2014).

1297 When using isolated mitochondria, total mitochondrial protein is a frequently applied
 1298 mitochondrial marker, the use of which is restricted to isolated mitochondria. The
 1299 mitochondrial recovery and yield, and experimental criteria for evaluation of purity versus
 1300 integrity should be reported. Mitochondrial markers—such as citrate synthase activity as an
 1301 enzymatic matrix marker—provide a link to the tissue of origin on the basis of calculating the
 1302 mitochondrial recovery, *i.e.*, the fraction of mitochondrial marker obtained from a unit mass of
 1303 tissue.
 1304

1305 **Box 3: Mitochondrial and cell respiration**

1306
 1307 Mitochondrial and cell respiration is the process of exergonic and exothermic energy
 1308 transformation in which scalar redox reactions are coupled to vectorial ion translocation across
 1309 a semipermeable membrane, which separates the small volume of a bacterial cell or
 1310 mitochondrion from the larger volume of its surroundings. The electrochemical exergy can be
 1311 partially conserved in the phosphorylation of ADP to ATP or in ion pumping, or dissipated in
 1312 an electrochemical short-circuit. Respiration is thus clearly distinguished from fermentation as
 1313 the counterpart of cellular core energy metabolism. Respiration is separated in mitochondrial
 1314 preparations from the partial contribution of fermentative pathways of the intact cell. Residual
 1315 oxygen consumption—as measured after inhibition of mitochondrial electron transfer—does
 1316 not belong to the class of catabolic reactions and is, therefore, subtracted from total oxygen
 1317 consumption to obtain baseline-corrected respiration.

1318
 1319 Terms and symbols are summarized in **Table 8**. Their use will facilitate transdisciplinary
 1320 communication and support further developments towards a consistent theory of bioenergetics
 1321 and mitochondrial physiology. Technical terms related to and defined with normal words can
 1322 be used as index terms in databases, support the creation of ontologies towards semantic
 1323 information processing (MitoPedia), and help in communicating analytical findings as
 1324 impactful data-driven stories. *‘Making data available without making it understandable may be*
 1325 *worse than not making it available at all’* (National Academies of Sciences, Engineering, and
 1326 Medicine 2018). This is a call to carefully contribute to FAIR principles (Findable, Accessible,
 1327 Interoperable, Reusable) for the sharing of scientific data.
 1328

1329 **Acknowledgements**

1330 We thank M. Beno for management assistance. Supported by COST Action CA15203
 1331 MitoEAGLE and K-Regio project MitoFit (E.G.).
 1332

1333 **Competing financial interests:** E.G. is founder and CEO of Oroboros Instruments, Innsbruck,
 1334 Austria.
 1335

1336 **5. References**

- 1337
 1338
 1339 Altmann R (1894) Die Elementarorganismen und ihre Beziehungen zu den Zellen. Zweite vermehrte Auflage.
 1340 Verlag Von Veit & Comp, Leipzig:160 pp.
 1341 Beard DA (2005) A biophysical model of the mitochondrial respiratory system and oxidative phosphorylation.
 1342 PLoS Comput Biol 1(4):e36.
 1343 Benda C (1898) Weitere Mitteilungen über die Mitochondria. Verh Dtsch Physiol Ges:376-83.
 1344 Birkedal R, Laasmaa M, Vendelin M (2014) The location of energetic compartments affects energetic
 1345 communication in cardiomyocytes. Front Physiol 5:376.

- 1346 Breton S, Beaupré HD, Stewart DT, Hoeh WR, Blier PU (2007) The unusual system of doubly uniparental
 1347 inheritance of mtDNA: isn't one enough? *Trends Genet* 23:465-74.
- 1348 Brown GC (1992) Control of respiration and ATP synthesis in mammalian mitochondria and cells. *Biochem J*
 1349 284:1-13.
- 1350 Calvo SE, Klausner CR, Mootha VK (2016) MitoCarta2.0: an updated inventory of mammalian mitochondrial
 1351 proteins. *Nucleic Acids Research* 44:D1251-7.
- 1352 Calvo SE, Julien O, Clauser KR, Shen H, Kamer KJ, Wells JA, Mootha VK (2017) Comparative analysis of
 1353 mitochondrial N-termini from mouse, human, and yeast. *Mol Cell Proteomics* 16:512-23.
- 1354 Campos JC, Queliconi BB, Bozi LHM, Bechara LRG, Dourado PMM, Andres AM, Jannig PR, Gomes KMS,
 1355 Zambelli VO, Rocha-Resende C, Guatimosim S, Brum PC, Mochly-Rosen D, Gottlieb RA, Kowaltowski AJ,
 1356 Ferreira JCB (2017) Exercise reestablishes autophagic flux and mitochondrial quality control in heart failure.
 1357 *Autophagy* 13:1304-317.
- 1358 Canton M, Luvisetto S, Schmehl I, Azzone GF (1995) The nature of mitochondrial respiration and
 1359 discrimination between membrane and pump properties. *Biochem J* 310:477-81.
- 1360 Chance B, Williams GR (1955a) Respiratory enzymes in oxidative phosphorylation. I. Kinetics of oxygen
 1361 utilization. *J Biol Chem* 217:383-93.
- 1362 Chance B, Williams GR (1955b) Respiratory enzymes in oxidative phosphorylation: III. The steady state. *J Biol*
 1363 *Chem* 217:409-27.
- 1364 Chance B, Williams GR (1955c) Respiratory enzymes in oxidative phosphorylation. IV. The respiratory chain. *J*
 1365 *Biol Chem* 217:429-38.
- 1366 Chance B, Williams GR (1956) The respiratory chain and oxidative phosphorylation. *Adv Enzymol Relat Subj*
 1367 *Biochem* 17:65-134.
- 1368 Cobb LJ, Lee C, Xiao J, Yen K, Wong RG, Nakamura HK, Mehta HH, Gao Q, Ashur C, Huffman DM, Wan J,
 1369 Muzumdar R, Barzilai N, Cohen P (2016) Naturally occurring mitochondrial-derived peptides are age-
 1370 dependent regulators of apoptosis, insulin sensitivity, and inflammatory markers. *Aging (Albany NY)* 8:796-
 1371 809.
- 1372 Cohen ER, Cvitas T, Frey JG, Holmström B, Kuchitsu K, Marquardt R, Mills I, Pavese F, Quack M, Stohner J,
 1373 Strauss HL, Takami M, Thor HL (2008) Quantities, units and symbols in physical chemistry, IUPAC Green
 1374 Book, 3rd Edition, 2nd Printing, IUPAC & RSC Publishing, Cambridge.
- 1375 Cooper H, Hedges LV, Valentine JC, eds (2009) *The handbook of research synthesis and meta-analysis*. Russell
 1376 Sage Foundation.
- 1377 Coopersmith J (2010) *Energy, the subtle concept. The discovery of Feynman's blocks from Leibnitz to Einstein*.
 1378 Oxford University Press:400 pp.
- 1379 Cummins J (1998) Mitochondrial DNA in mammalian reproduction. *Rev Reprod* 3:172-82.
- 1380 Dai Q, Shah AA, Garde RV, Yonish BA, Zhang L, Medvitz NA, Miller SE, Hansen EL, Dunn CN, Price TM
 1381 (2013) A truncated progesterone receptor (PR-M) localizes to the mitochondrion and controls cellular
 1382 respiration. *Mol Endocrinol* 27:741-53.
- 1383 Divakaruni AS, Brand MD (2011) The regulation and physiology of mitochondrial proton leak. *Physiology*
 1384 (Bethesda) 26:192-205.
- 1385 Doerrier C, Garcia-Souza LF, Krumschnabel G, Wohlfarter Y, Mészáros AT, Gnaiger E (2018) High-Resolution
 1386 FluoRespirometry and OXPHOS protocols for human cells, permeabilized fibres from small biopsies of
 1387 muscle and isolated mitochondria. *Methods Mol. Biol.* (in press)
- 1388 Doskey CM, van 't Erve TJ, Wagner BA, Buettner GR (2015) Moles of a substance per cell is a highly
 1389 informative dosing metric in cell culture. *PLOS ONE* 10:e0132572.
- 1390 Drahota Z, Milerová M, Stieglerová A, Houstek J, Ostádal B (2004) Developmental changes of cytochrome *c*
 1391 oxidase and citrate synthase in rat heart homogenate. *Physiol Res* 53:119-22.
- 1392 Duarte FV, Palmeira CM, Rolo AP (2014) The role of microRNAs in mitochondria: small players acting wide.
 1393 *Genes (Basel)* 5:865-86.
- 1394 Ernster L, Schatz G (1981) Mitochondria: a historical review. *J Cell Biol* 91:227s-55s.
- 1395 Estabrook RW (1967) Mitochondrial respiratory control and the polarographic measurement of ADP:O ratios.
 1396 *Methods Enzymol* 10:41-7.
- 1397 Faber C, Zhu ZJ, Castellino S, Wagner DS, Brown RH, Peterson RA, Gates L, Barton J, Bickett M, Hagerty L,
 1398 Kimbrough C, Sola M, Bailey D, Jordan H, Elangbam CS (2014) Cardiolipin profiles as a potential
 1399 biomarker of mitochondrial health in diet-induced obese mice subjected to exercise, diet-restriction and
 1400 ephedrine treatment. *J Appl Toxicol* 34:1122-9.
- 1401 Fell D (1997) *Understanding the control of metabolism*. Portland Press.
- 1402 Garlid KD, Beavis AD, Ratkje SK (1989) On the nature of ion leaks in energy-transducing membranes. *Biochim*
 1403 *Biophys Acta* 976:109-20.
- 1404 Garlid KD, Semrad C, Zinchenko V. Does redox slip contribute significantly to mitochondrial respiration? In:
 1405 Schuster S, Rigoulet M, Ouhabi R, Mazat J-P, eds (1993) *Modern trends in biothermokinetics*. Plenum Press,
 1406 New York, London:287-93.

- 1407 Gerö D, Szabo C (2016) Glucocorticoids suppress mitochondrial oxidant production via upregulation of
 1408 uncoupling protein 2 in hyperglycemic endothelial cells. *PLoS One* 11:e0154813.
- 1409 Gnaiger E. Efficiency and power strategies under hypoxia. Is low efficiency at high glycolytic ATP production a
 1410 paradox? In: *Surviving Hypoxia: Mechanisms of Control and Adaptation*. Hochachka PW, Lutz PL, Sick T,
 1411 Rosenthal M, Van den Thillart G, eds (1993a) CRC Press, Boca Raton, Ann Arbor, London, Tokyo:77-109.
- 1412 Gnaiger E (1993b) Nonequilibrium thermodynamics of energy transformations. *Pure Appl Chem* 65:1983-2002.
- 1413 Gnaiger E (2001) Bioenergetics at low oxygen: dependence of respiration and phosphorylation on oxygen and
 1414 adenosine diphosphate supply. *Respir Physiol* 128:277-97.
- 1415 Gnaiger E (2009) Capacity of oxidative phosphorylation in human skeletal muscle. New perspectives of
 1416 mitochondrial physiology. *Int J Biochem Cell Biol* 41:1837-45.
- 1417 Gnaiger E (2014) Mitochondrial pathways and respiratory control. An introduction to OXPHOS analysis. 4th ed.
 1418 *Mitochondr Physiol Network* 19.12. Oroboros MiPNet Publications, Innsbruck:80 pp.
- 1419 Gnaiger E, Méndez G, Hand SC (2000) High phosphorylation efficiency and depression of uncoupled respiration
 1420 in mitochondria under hypoxia. *Proc Natl Acad Sci USA* 97:11080-5.
- 1421 Greggio C, Jha P, Kulkarni SS, Lagarrigue S, Broskey NT, Boutant M, Wang X, Conde Alonso S, Ofori E,
 1422 Auwerx J, Cantó C, Amati F (2017) Enhanced respiratory chain supercomplex formation in response to
 1423 exercise in human skeletal muscle. *Cell Metab* 25:301-11.
- 1424 Hinkle PC (2005) P/O ratios of mitochondrial oxidative phosphorylation. *Biochim Biophys Acta* 1706:1-11.
- 1425 Hofstadter DR (1979) Gödel, Escher, Bach: An eternal golden braid. A metaphorical fugue on minds and
 1426 machines in the spirit of Lewis Carroll. Harvester Press:499 pp.
- 1427 Illaste A, Laasmaa M, Peterson P, Vendelin M (2012) Analysis of molecular movement reveals latticelike
 1428 obstructions to diffusion in heart muscle cells. *Biophys J* 102:739-48.
- 1429 Jasienski M, Bazzaz FA (1999) The fallacy of ratios and the testability of models in biology. *Oikos* 84:321-26.
- 1430 Jepihina N, Beraud N, Sepp M, Birkedal R, Vendelin M (2011) Permeabilized rat cardiomyocyte response
 1431 demonstrates intracellular origin of diffusion obstacles. *Biophys J* 101:2112-21.
- 1432 Klepinin A, Ounpuu L, Guzun R, Chekulayev V, Timohhina N, Tepp K, Shevchuk I, Schlattner U, Kaambre T
 1433 (2016) Simple oxygraphic analysis for the presence of adenylate kinase 1 and 2 in normal and tumor cells. *J*
 1434 *Bioenerg Biomembr* 48:531-48.
- 1435 Klingenberg M (2017) UCP1 - A sophisticated energy valve. *Biochimie* 134:19-27.
- 1436 Koit A, Shevchuk I, Ounpuu L, Klepinin A, Chekulayev V, Timohhina N, Tepp K, Puurand M, Truu L, Heck K,
 1437 Valvere V, Guzun R, Kaambre T (2017) Mitochondrial respiration in human colorectal and breast cancer
 1438 clinical material is regulated differently. *Oxid Med Cell Longev* 1372640.
- 1439 Komlódi T, Tretter L (2017) Methylene blue stimulates substrate-level phosphorylation catalysed by succinyl-
 1440 CoA ligase in the citric acid cycle. *Neuropharmacology* 123:287-98.
- 1441 Lane N (2005) Power, sex, suicide: mitochondria and the meaning of life. Oxford University Press:354 pp.
- 1442 Larsen S, Nielsen J, Neigaard Nielsen C, Nielsen LB, Wibrand F, Stride N, Schroder HD, Boushel RC, Helge
 1443 JW, Dela F, Hey-Mogensen M (2012) Biomarkers of mitochondrial content in skeletal muscle of healthy
 1444 young human subjects. *J Physiol* 590:3349-60.
- 1445 Lee C, Zeng J, Drew BG, Sallam T, Martin-Montalvo A, Wan J, Kim SJ, Mehta H, Hevener AL, de Cabo R,
 1446 Cohen P (2015) The mitochondrial-derived peptide MOTS-c promotes metabolic homeostasis and reduces
 1447 obesity and insulin resistance. *Cell Metab* 21:443-54.
- 1448 Lee SR, Kim HK, Song IS, Youm J, Dizon LA, Jeong SH, Ko TH, Heo HJ, Ko KS, Rhee BD, Kim N, Han J
 1449 (2013) Glucocorticoids and their receptors: insights into specific roles in mitochondria. *Prog Biophys Mol*
 1450 *Biol* 112:44-54.
- 1451 Leek BT, Mudaliar SR, Henry R, Mathieu-Costello O, Richardson RS (2001) Effect of acute exercise on citrate
 1452 synthase activity in untrained and trained human skeletal muscle. *Am J Physiol Regul Integr Comp Physiol*
 1453 280:R441-7.
- 1454 Lemieux H, Blier PU, Gnaiger E (2017) Remodeling pathway control of mitochondrial respiratory capacity by
 1455 temperature in mouse heart: electron flow through the Q-junction in permeabilized fibers. *Sci Rep* 7:2840.
- 1456 Lenaz G, Tioli G, Falasca AI, Genova ML (2017) Respiratory supercomplexes in mitochondria. In: *Mechanisms*
 1457 *of primary energy trasduction in biology*. M Wikstrom (ed) Royal Society of Chemistry Publishing, London,
 1458 UK:296-337.
- 1459 Margulis L (1970) Origin of eukaryotic cells. New Haven: Yale University Press.
- 1460 Meinild Lundby AK, Jacobs RA, Gehrig S, de Leur J, Hauser M, Bonne TC, Flück D, Dandanell S, Kirk N,
 1461 Kaech A, Ziegler U, Larsen S, Lundby C (2018) Exercise training increases skeletal muscle mitochondrial
 1462 volume density by enlargement of existing mitochondria and not de novo biogenesis. *Acta Physiol* 222,
 1463 e12905.
- 1464 Menshikova EV, Ritov VB, Fairfull L, Ferrell RE, Kelley DE, Goodpaster BH (2006) Effects of exercise on
 1465 mitochondrial content and function in aging human skeletal muscle. *J Gerontol A Biol Sci Med Sci* 61:534-
 1466 40.

- 1467 Menshikova EV, Ritov VB, Ferrell RE, Azuma K, Goodpaster BH, Kelley DE (2007) Characteristics of skeletal
 1468 muscle mitochondrial biogenesis induced by moderate-intensity exercise and weight loss in obesity. *J Appl*
 1469 *Physiol* (1985) 103:21-7.
- 1470 Menshikova EV, Ritov VB, Toledo FG, Ferrell RE, Goodpaster BH, Kelley DE (2005) Effects of weight loss
 1471 and physical activity on skeletal muscle mitochondrial function in obesity. *Am J Physiol Endocrinol Metab*
 1472 288:E818-25.
- 1473 Miller GA (1991) *The science of words*. Scientific American Library New York:276 pp.
- 1474 Mitchell P (1961) Coupling of phosphorylation to electron and hydrogen transfer by a chemi-osmotic type of
 1475 mechanism. *Nature* 191:144-8.
- 1476 Mitchell P (2011) Chemiosmotic coupling in oxidative and photosynthetic phosphorylation. *Biochim Biophys*
 1477 *Acta Bioenergetics* 1807:1507-38.
- 1478 Mogensen M, Sahlin K, Fernström M, Glintborg D, Vind BF, Beck-Nielsen H, Højlund K (2007) Mitochondrial
 1479 respiration is decreased in skeletal muscle of patients with type 2 diabetes. *Diabetes* 56:1592-9.
- 1480 Mohr PJ, Phillips WD (2015) Dimensionless units in the SI. *Metrologia* 52:40-7.
- 1481 Moreno M, Giacco A, Di Munno C, Goglia F (2017) Direct and rapid effects of 3,5-diiodo-L-thyronine (T2).
 1482 *Mol Cell Endocrinol* 7207:30092-8.
- 1483 Morrow RM, Picard M, Derbeneva O, Leipzig J, McManus MJ, Gousspillou G, Barbat-Artigas S, Dos Santos C,
 1484 Hepple RT, Murdock DG, Wallace DC (2017) Mitochondrial energy deficiency leads to hyperproliferation of
 1485 skeletal muscle mitochondria and enhanced insulin sensitivity. *Proc Natl Acad Sci U S A* 114:2705-10.
- 1486 Murley A, Nunnari J (2016) The emerging network of mitochondria-organelle contacts. *Mol Cell* 61:648-53.
- 1487 National Academies of Sciences, Engineering, and Medicine (2018) International coordination for science data
 1488 infrastructure: Proceedings of a workshop—in brief. Washington, DC: The National Academies Press. doi:
 1489 <https://doi.org/10.17226/25015>.
- 1490 Paradies G, Paradies V, De Benedictis V, Ruggiero FM, Petrosillo G (2014) Functional role of cardiolipin in
 1491 mitochondrial bioenergetics. *Biochim Biophys Acta* 1837:408-17.
- 1492 Pesta D, Gnaiger E (2012) High-Resolution Respirometry. OXPHOS protocols for human cells and
 1493 permeabilized fibres from small biopsies of human muscle. *Methods Mol Biol* 810:25-58.
- 1494 Pesta D, Hoppel F, Macek C, Messner H, Faulhaber M, Kobel C, Parson W, Burtscher M, Schocke M, Gnaiger
 1495 E (2011) Similar qualitative and quantitative changes of mitochondrial respiration following strength and
 1496 endurance training in normoxia and hypoxia in sedentary humans. *Am J Physiol Regul Integr Comp Physiol*
 1497 301:R1078–87.
- 1498 Price TM, Dai Q (2015) The role of a mitochondrial progesterone receptor (PR-M) in progesterone action.
 1499 *Semin Reprod Med* 33:185-94.
- 1500 Puchowicz MA, Varnes ME, Cohen BH, Friedman NR, Kerr DS, Hoppel CL (2004) Oxidative phosphorylation
 1501 analysis: assessing the integrated functional activity of human skeletal muscle mitochondria – case studies.
 1502 *Mitochondrion* 4:377-85. Puntschart A, Claassen H, Jostarnndt K, Hoppeler H, Billeter R (1995) mRNAs of
 1503 enzymes involved in energy metabolism and mtDNA are increased in endurance-trained athletes. *Am J*
 1504 *Physiol* 269:C619-25.
- 1505 Quiros PM, Mottis A, Auwerx J (2016) Mitonuclear communication in homeostasis and stress. *Nat Rev Mol*
 1506 *Cell Biol* 17:213-26.
- 1507 Reichmann H, Hoppeler H, Mathieu-Costello O, von Bergen F, Pette D (1985) Biochemical and ultrastructural
 1508 changes of skeletal muscle mitochondria after chronic electrical stimulation in rabbits. *Pflugers Arch* 404:1-
 1509 9.
- 1510 Renner K, Amberger A, Konwalinka G, Gnaiger E (2003) Changes of mitochondrial respiration, mitochondrial
 1511 content and cell size after induction of apoptosis in leukemia cells. *Biochim Biophys Acta* 1642:115-23.
- 1512 Rich P (2003) Chemiosmotic coupling: The cost of living. *Nature* 421:583.
- 1513 Rostovtseva TK, Sheldon KL, Hassanzadeh E, Monge C, Saks V, Bezrukov SM, Sackett DL (2008) Tubulin
 1514 binding blocks mitochondrial voltage-dependent anion channel and regulates respiration. *Proc Natl Acad Sci*
 1515 *USA* 105:18746-51.
- 1516 Rustin P, Parfait B, Chretien D, Bourgeron T, Djouadi F, Bastin J, Rötig A, Munnich A (1996) Fluxes of
 1517 nicotinamide adenine dinucleotides through mitochondrial membranes in human cultured cells. *J Biol Chem*
 1518 271:14785-90.
- 1519 Saks VA, Veksler VI, Kuznetsov AV, Kay L, Sikk P, Tiivel T, Tranqui L, Olivares J, Winkler K, Wiedemann F,
 1520 Kunz WS (1998) Permeabilised cell and skinned fiber techniques in studies of mitochondrial function in
 1521 vivo. *Mol Cell Biochem* 184:81-100.
- 1522 Salabei JK, Gibb AA, Hill BG (2014) Comprehensive measurement of respiratory activity in permeabilized cells
 1523 using extracellular flux analysis. *Nat Protoc* 9:421-38.
- 1524 Sazanov LA (2015) A giant molecular proton pump: structure and mechanism of respiratory complex I. *Nat Rev*
 1525 *Mol Cell Biol* 16:375-88.
- 1526 Schneider TD (2006) Claude Shannon: biologist. The founder of information theory used biology to formulate
 1527 the channel capacity. *IEEE Eng Med Biol Mag* 25:30-3.

- 1528 Schönfeld P, Dymkowska D, Wojtczak L (2009) Acyl-CoA-induced generation of reactive oxygen species in
1529 mitochondrial preparations is due to the presence of peroxisomes. *Free Radic Biol Med* 47:503-9.
- 1530 Schultz J, Wiesner RJ (2000) Proliferation of mitochondria in chronically stimulated rabbit skeletal muscle--
1531 transcription of mitochondrial genes and copy number of mitochondrial DNA. *J Bioenerg Biomembr* 32:627-
1532 34.
- 1533 Simson P, Jepihhina N, Laasmaa M, Peterson P, Birkedal R, Vendelin M (2016) Restricted ADP movement in
1534 cardiomyocytes: Cytosolic diffusion obstacles are complemented with a small number of open mitochondrial
1535 voltage-dependent anion channels. *J Mol Cell Cardiol* 97:197-203.
- 1536 Stucki JW, Ineichen EA (1974) Energy dissipation by calcium recycling and the efficiency of calcium transport
1537 in rat-liver mitochondria. *Eur J Biochem* 48:365-75.
- 1538 Tonkonogi M, Harris B, Sahlin K (1997) Increased activity of citrate synthase in human skeletal muscle after a
1539 single bout of prolonged exercise. *Acta Physiol Scand* 161:435-6.
- 1540 Waczulikova I, Habodaszova D, Cagalinec M, Ferko M, Ulicna O, Mateasik A, Sikurova L, Ziegelhöffer A
1541 (2007) Mitochondrial membrane fluidity, potential, and calcium transients in the myocardium from acute
1542 diabetic rats. *Can J Physiol Pharmacol* 85:372-81.
- 1543 Wagner BA, Venkataraman S, Buettner GR (2011) The rate of oxygen utilization by cells. *Free Radic Biol Med*
1544 51:700-712.
- 1545 Wang H, Hiatt WR, Barstow TJ, Brass EP (1999) Relationships between muscle mitochondrial DNA content,
1546 mitochondrial enzyme activity and oxidative capacity in man: alterations with disease. *Eur J Appl Physiol*
1547 *Occup Physiol* 80:22-7.
- 1548 Watt IN, Montgomery MG, Runswick MJ, Leslie AG, Walker JE (2010) Bioenergetic cost of making an
1549 adenosine triphosphate molecule in animal mitochondria. *Proc Natl Acad Sci U S A* 107:16823-7.
- 1550 Weibel ER, Hoppeler H (2005) Exercise-induced maximal metabolic rate scales with muscle aerobic capacity. *J*
1551 *Exp Biol* 208:1635-44.
- 1552 White DJ, Wolff JN, Pierson M, Gemmell NJ (2008) Revealing the hidden complexities of mtDNA inheritance.
1553 *Mol Ecol* 17:4925-42.
- 1554 Wikström M, Hummer G (2012) Stoichiometry of proton translocation by respiratory complex I and its
1555 mechanistic implications. *Proc Natl Acad Sci U S A* 109:4431-6.
- 1556 Willis WT, Jackman MR, Messer JI, Kuzmiak-Glancy S, Glancy B (2016) A simple hydraulic analog model of
1557 oxidative phosphorylation. *Med Sci Sports Exerc* 48:990-1000.